from previous studies using multi-channel systems, which indicated that maximum activation in the PFC corresponded to Fp1-Fp7 and Fp2-Fp8 locations, where the probes were placed for our measurements (Takizawa et al., 2008; Ehlis et al., 2008; Kubota et al., 2005; Watanabe and Kato, 2004; Suto et al., 2004). In both schizophrenia and healthy control groups, task performance was found to be better for VFT-category than for VFT-letter, whereas task-induced Δ[oxyHb] were found to be larger during VFT-letter than during VFT-category. In particular, a group difference was more apparent for VFT-letter than VFT-category, which is in line with recent findings by Ehlis et al. (2008). With regard to the retrieval of words during VFT-letter, the task may require larger cognitive demands, as the letter version has been reported unfamiliar to subjects compared to the category version (Martin et al., 1994). This may explain in part why performance of the category-version was better than performance of the letter-version, and Δ[oxyHb] during the letter-version task was larger than that during the category version. In addition, pronounced phonological (letter fluency) deficits in schizophrenia patients (Ehlis et al., 2008; Curtis et al., 1999) may also account for the difference between schizophrenia patients and healthy controls regarding Δ[oxyHb] during VFT-letter. Thus, VFT-letter appears to be more appropriate than VFT-category when screening for prefrontal dysfunction in schizophrenia.

As for TOH, several studies have reported PFC activation. For instance, activation in the right dorsolateral PFC, bilateral parietal, bilateral premotor area, and the left inferior frontal gyrus was reported in normal subjects using fMRI (Fincham et al., 2002). Findings from studies of patients with PFC lesions have proposed that this cortical area plays a crucial role in the execution of TOH (Morris et al., 1997; Goel and Grafman, 1995). Since no neuroimaging studies using TOH have been reported in schizophrenia, an accurate location of the peak of activation remains to be determined. However, the behavior of Δ[oxyHb] in this study was almost identical during TOH and VFT-letter, the means of Δ[oxyHb] in healthy controls were larger for TOH (left: 1.78 ± 1.16, right: 1.77 ± 1.22) than for VFT-letter (left: 1.58 ± 1.01, right: 1.58 ± 1.01), and the effect size of Δ[oxyHb] between healthy controls and schizophrenia patients was larger for TOH (left: 0.90, right: 0.86) than for VFT-letter (left: 0.82, right: 0.88). These reflect the validity of measurements with a 2ch-NIRS system in limited cortical areas like those corresponding to Fp1–Fp7 and Fp2–Fp8. In the present study, there was significant interaction between diagnosis group and gender only for TOH, with male healthy controls showing larger activation than schizophrenia patients. Despite evidence of clinical and biological differences in schizophrenia, particularly in structural brain abnormalities (Nasrallah et al., 1990), specific functional changes in the brain of schizophrenia patients during cognitive tasks in relation to gender have not been reported (Buchsbaum and Hazlett, 1997). Thus, gender difference in cortical activation in schizophrenia needs further investigation.

With regard to the Sternberg task, the measurement areas in this study corresponded well with locations exhibiting significant task-induced activation and significant difference by diagnosis in a previous fMRI study (Johnson et al., 2006). However, no significant difference in Δ[oxyHb] was observed between schizophrenia patients and healthy controls in this study. A number of methodological differences between our study and previous investigations may explain partly the discrepancy in the findings. Firstly, the presence of variability in activation size due to working memory load and diagnosis group effect may account for the difference in the findings. In this regard, previous fMRI studies reported that the relation between activation size and working memory load of the Sternberg task exhibited an inverse U-curve, and that the difference of activation between schizophrenia patients and healthy controls was the smallest when working memory load consisted of a 5-digit paradigm (Johnson et al., 2006; Manoach, 2003), which we used in this study. Secondly, we should consider the differences in data analyses: in previous fMRI studies, the encoding phase and the delay phase were analyzed separately, resulting in significant difference in activation for each phase (Schlösser et al., 2008; Johnson et al., 2006). Since our analyses do not allow phases discrimination, significant findings for each phase cannot be determined in the present study. Thirdly, in the Sternberg task in this study, the encoding and delay phases were comparatively shorter than those used in other studies (Schlösser et al., 2008; Johnson et al., 2006). This might also obscure significant differences in activation. The Stroop task has also been employed in previous PET and fMRI studies where it indicated strong anterior cingulate cortex activation (Alvarez and Emory, 2006). A NIRS study conducted with healthy subjects found a significant increase in Δ[oxyHb] in the left inferior-frontal area induced by the Stroop task (Ehlis et al., 2005). This location was somewhat posterior to our measurement position. Thus, although the main purpose of this study was comprehensive assessment of multiple frontal lobe functions using a 2ch-NIRS system, our measurement position might be outside of the major significant activations induced by the Stroop task. Moreover, recent reports suggest that evident activation is associated with the presentation of incongruent stimuli only (Ehlis et al., 2005; Kerns et al., 2005). However, the analyses used in our study do not allow us to distinguish incongruent from congruent stimuli. Furthermore, Boucart et al. (1999) reported that the main alteration evident during the Stroop task for schizophrenia patients was recognized when the words were surrounded by others. In this study, single words were presented on-screen, one at a time. Thus, we cannot rule out the possibility that group difference in Δ[oxyHb] could have been found, if we employed the paradigm by Boucart et al. (1999). Limitations in analysis methods may hence account for the lack of Stroop task-induced activation in this study.

As for the effect of the task order, we found that task order was relevant in VFT-letter and the Stroop task. As a result of the design-1 ANCOVA, mean activation values were larger during order A than during order B in VFT letter for both groups. However, mean activation values were larger during order B than during order A in the Stroop task for both groups. Because activation values collected in the latter line of experiments decreased, we concluded that a lower number of tasks and a short time of tasks were most appropriate in clinical examinations.

In the present study, we attempted to relate demographic and major clinical parameters to Δ[oxyHb] during performance of those tasks showing significant diagnosis group difference (i.e., VFT-letter and TOH). For both schizophrenia and healthy control groups, Δ[oxyHb] did not correlate with

either age or level of performance. In schizophrenia patients, left Δ[oxyHb] during TOH correlated positively with JART, and inversely with illness duration. These findings support that a higher premorbid IQ correlates with larger activation in the left PFC, while longer illness predicts smaller activation in the same area. In healthy controls, right Δ[oxyHb] during TOH correlated positively with years of education. These data associate higher education with larger activation in the right PFC, which does not hold true in schizophrenia patients. We also tested for a correlation between clinical parameters and Δ[oxyHb] during VFT-letter and TOH in which significant diagnosis group effects were observed. During TOH, we found a significant negative correlation of left Δ[oxyHb] with negative symptoms scores on PANSS as well as negative and cognitive symptoms scores on the five-factor model of PANSS for schizophrenia patients. However, no significant correlation was found during VFT-letter. A negative correlation between executive function and negative symptoms scores on PANSS or cognitive symptoms scores on the five-factor model of PANSS has been previously reported in schizophrenia (Heydebrand et al., 2004; Bell et al., 1994). Our finding of a significant negative correlation between Δ[oxyHb] and negative symptoms scores is consistent with that of these earlier studies and with a report of decreased regional cerebral blood volume in PFC in schizophrenia patients with severe negative symptoms (Gonul et al., 2003). If Δ[oxyHb] correlates with negative and cognitive symptoms scores, specific Δ[oxyHb] induced by TOH, as demonstrated by 2ch-NIRS, may be used as a physiological state marker of schizophrenia. VFT-letter, however, showed significant differences in Δ[oxyHb] between schizophrenia and healthy controls, but no correlation between Δ[oxyHb] and clinical parameters, including negative and cognitive symptoms. Upon confirmation of this finding, Δ[oxyHb] induced by VFT-letter might constitute a potential physiological marker of the disease. In summary, multiple comparisons showed that correlations between Δ[oxyHb] and demographic and clinical parameters in schizophrenia during TOH cannot be deemed significant; albeit, these correlations may hold some meaning.

4.2. DeoxyHb data

Although [deoxyHb] has been considered mostly related to fMRI BOLD signal, some researchers emphasize that [deoxyHb] and [oxyHb] may index neural activation. While decrease in Δ[deoxyHb] during neural activation is typical, Δ[deoxyHb] behavior is in fact more complex. In simultaneous measurements of fMRI and NIRS, some studies report an increase in the BOLD signal, positively related to an increase in [oxyHb] in NIRS (Mehagnoul-Schipper et al., 2002; Toronov et al., 2001; Kleinschmidt et al., 1996). Others found an increase in the BOLD signal, positively related to a decrease in [deoxyHb] in NIRS (Strangman et al., 2002). Furthermore, BOLD signal increase in the area where neural activity was anticipated is sometimes not accompanied by [deoxyHb] decrease (Yamamoto and Kato, 2002). The BOLD signal is therefore not a reliable predictor of [deoxyHb]. As an index of neural activation, Δ[oxyHb] may be suitable, owing to the highest sensitivity amongst the NIRS parameters (Hoshi et al., 2001; Hoshi, 2003). We therefore weighted the results of [deoxyHb] as less important than those of [oxyHb], since the interpretation of [deoxyHb] in NIRS measurement has not been established yet.

The results of the analysis of Δ[deoxyHb] in this study indicated a significant main effect of the diagnosis group was in VFT-category, TOH and the Sternberg task. A significant interaction between diagnosis group and gender was recognized in TOH. A significant effect of task order was recognized in the Stroop task. In TOH, a significant decrease in Δ[deoxyHb] as well as increase in Δ[oxyHb] could be interpreted as significant group difference in the prefrontal activation. However, the results of Δ[deoxyHb] in VFT-category, the Sternberg task, and the Stroop task are difficult to interpret because these three tasks did not show significant differences in Δ[oxyHb].

4.3. Limitations

Our study is subject to several limitations. Since this is a cross-sectional study we cannot be sure that Δ[oxyHb] during TOH and VFT-letter are reliable physiological markers of schizophrenia. Longitudinal studies are necessary. A second limitation lies in the effect of optical path length factor on estimated Δ[oxyHb]. Although the optical path length may vary across individuals, we set the optical path length factor at 24 cm in the present study. Calculations of [oxyHb] and [deoxyHb] were based on the modified Beer–Lambert law, where

$$\Delta OD = \varepsilon(\lambda)*\Delta c*d*B,$$

with ΔOD being the change in absorbance, $\varepsilon(\lambda)$ is the molar absorbance efficient, Δc is the change in the concentration of absorbed materials, d is the distance between optical probes, and B is the differential path length factor. The optical path length ($d*B$) of each subject is needed for quantitative estimation. This requires the assumption that optical path length factors are constant among positions and individuals. Nevertheless, studies using time-resolved spectroscopy methods of NIRS have reported no difference in the path length due to diagnosis (schizophrenia and healthy controls) and laterality (at Fp1-F7 and Fp2-F8), as well as at most 20% path length variability among positions and individuals (Shinba et al., 2004), which could produce about 20% variability in estimated Δ[oxyHb] according to the formula. This Δ[oxyHb] variability corresponds to 20–30% of its standard deviation. If assumed to be noise, the standard deviation of estimated Δ[oxyHb] increases thus lowering the effect sizes, although the effect sizes of Δ[oxyHb] during VFT-letter and TOH were sufficiently large (>0.8). The effect size of Δ[oxyHb] would hence be greater than 0.8 in absence of inter-individual variability of the optical path length when estimating Δ[oxyHb]. Furthermore, taking into account the significant differences in Δ[oxyHb] during VFT-letter and TOH, and the lack of difference during the Stroop task in the present study, we consider that the group difference between schizophrenia patients and healthy controls in our study could not be affected by the path length factor. As measures of the optical path length factor become easier with technological advances, and quantitative accuracy of Δ[oxyHb] improves, the potential clinical application of Δ[oxyHb] may dramatically increase. A third limitation is the potential influence of

antipsychotic medications and benzodiazepines (BZD) on Δ[oxyHb]. A negative correlation was observed between right Δ[oxyHb] and CPZ equivalents during TOH, while no correlation was observed between left Δ[oxyHb] and CPZ equivalents during either TOH or VFT-letter in this study. We do not have a clear explanation for this finding at the present time. Cognitive improvement in schizophrenia has been reported in association with atypical rather than typical antipsychotics (Keefe et al., 1999). The interpretation of the influence of antipsychotics in this study is complicated by the concomitant use of typical and atypical antipsychotics in some patients. Since BZD affects rCBF (Reinsel et al., 2000), we performed further analyses to divide the schizophrenia group into two subgroups, BZD-on group and BZD-off group, to test for possible differences in Δ[oxyHb] between the two subgroups, but none were found (data were not shown). Therefore, we conclude our present results were not influenced by BZD.

4.4. Conclusions

In summary, we have examined hemodynamic changes in [oxyHb] in the bilateral PFC in schizophrenia patients and healthy controls using a 2ch-NIRS system during several cognitive tasks. VFT-letter and TOH appear to offer a better discriminative power than other neuropsychological tests to recognize PFC dysfunction in schizophrenia patients. In addition, Δ[oxyHb] in the left PFC correlated with negative and cognitive symptoms. This finding proposes that TOH and VFT-letter elicit PFC hemodynamic changes which might represent candidate physiological markers of schizophrenia. Despite the limitations of our study, we conclude that the 2ch-NIRS has potential for PFC activity measurements not only in schizophrenia patients, but also in other psychiatric disorders owing to several advantages such as simplicity and low running cost.

Role of funding source

Funding for this study was provided by Grants-in-Aid from the Japanese Ministry of Health, Labor and Welfare (H19-kokoro-002), the Japanese Ministry of Education, Culture, Sports, Science and Technology (17191211, 18689030, 18023045, 20591402); the Japanese Ministry of Health, Labor and Welfare, the Japanese Ministry of Education, Culture, Sports, Science and Technology had no further role in the study design; in the collection, analysis and interpretation of data; in the writing of the report; and in the decision to submit the paper for publication.

Contributors

K.I. and M.I. designed the study and wrote the protocol and undertook the statistical analysis. K.I., M.A., K.O., Y.Y., N.I., H.T., R.S., and T.Y. conducted data acquisition. K.I. and M.I. analyzed the data. K.I. wrote the first draft of the manuscript. L.C., R.K., T.N., and R.I. contributed to the editing of the final manuscript. All authors revised it critically for important intellectual content and have approved the final manuscript. R.H., H.K., and M.T. supervised the entire project.

Conflict of interest

None.

Acknowledgements

We deeply thank Mr. Christoph Lossin who checked our manuscript, and also thank Mrs. Koyama and Miss Kiribayashi, who kindly assisted with the preparation of our study.

References

Alvarez, J.A., Emory, E., 2006. Executive function and the frontal lobes: a meta-analytic review. Neuropsychol. Rev. 16, 17–42.

American Psychiatric Association, 1994. Diagnostic and Statistical Manual of Mental Disorders, Fourth Edition. American Psychiatric Association, Washington, DC.

Bell, M.D., Lysaker, P.H., Milstein, R.M., Beam-Goulet, J.L., 1994. Concurrent validity of the cognitive component of schizophrenia: relationship of PANSS scores to neuropsychological assessments. Psychiatry Res. 54, 51–58.

Boucart, M., Mobarek, N., Cuervo, C., Danion, J.M., 1999. What is the nature of increased Stroop interference in schizophrenia? Acta Psychol. 101, 3–25.

Buchsbaum, M.S., Hazlett, E.A., 1997. Update on PET glucose neuroimaging. Int. Rev. Psychiatry 20, 396–404.

Casement, M.D., Broussard, J.L., Mullington, J.M., Press, D.Z., 2006. The contribution of sleep to improvements in working memory scanning speed: a study of prolonged sleep restriction. Biol. Psychol. 72, 208–212.

Curtin, F., Schulz, P., 1998. Multiple correlations and Bonferroni's correction. Biol. Psychiatry 44, 775–777.

Curtis, V.A., Bullmore, E.T., Morris, R.G., Brammer, M.J., Williams, S.C., Simmons, A., Sharma, T., Murray, R.M., McGuire, P.K., 1999. Attenuated frontal activation in schizophrenia may be task dependent. Schizophr. Res. 37, 35–44.

Ehlis, A.C., Herrmann, M.J., Wagener, A., Fallgatter, A.J., 2005. Multi-channel near-infrared spectroscopy detects specific inferior-frontal activation during incongruent Stroop trials. Biol. Psychol. 69, 315–331.

Ehlis, A.C., Bähne, C.G., Jacob, C.P., Herrmann, M.J., Fallgatter, A.J., 2008. Reduced lateral prefrontal activation in adult patients with attention-deficit/hyperactivity disorder (ADHD) during a working memory task: a functional near-infrared spectroscopy (fNIRS) study. J. Psychiatr. Res. 42, 1060–1067.

Fallgatter, A.J., Strik, W.K., 2000. Reduced frontal functional asymmetry in schizophrenia during a cued continuous performance test assessed with near-infrared spectroscopy. Schizophr. Bull. 26, 913–919.

Fallgatter, A.J., Roesler, M., Sitzmann, L., Heidrich, A., Msueller, T.J., Strik, W.K., 1997. Loss of functional hemispheric asymmetry in Alzheimer's dementia assessed with near-infrared spectroscopy. Brain Res. Cogn. Brain Res. 6, 67–72.

Fincham, J.M., Carter, C.S., van Veen, V., Stenger, V.A., Anderson, J.R., 2002. Neural mechanisms of planning: a computational analysis using event-related fMRI. Proc. Natl. Acad. Sci. 99, 3346–3351.

Folley, B.S., Park, S., 2005. Verbal creativity and schizotypal personality in relation to prefrontal hemispheric laterality: a behavioral and near-infrared optical imaging study. Schizophr. Res. 15, 271–282.

Fox, P.T., Raichle, M.E., 1986. Focal physiological uncoupling of cerebral blood flow and oxidative metabolism during somatosensory stimulation in human subjects. Proc. Natl. Acad. Sci. 83, 1140–1144.

Giménez, M., Junqué, C., Pérez, M., Vendrell, P., Baeza, I., Salamero, M., Mercader, J.M., Bernardo, M., 2003. Basal ganglia N-acetylaspartate correlates with the performance in the procedural task 'Tower of Hanoi' of neuroleptic-naive schizophrenic patients. Neurosci. Lett. 347, 97–100.

Goel, V., Grafman, J., 1995. Are the frontal lobes implicated in "planning" functions? Interpreting data from the Tower of Hanoi. Neuropsychologia 33, 623–642.

Gonul, A.S., Kula, M., Eşel, E., Tutuş, A., Sofuoglu, S., 2003. A Tc-99m HMPAO SPECT study of regional cerebral blood flow in drug-free schizophrenic patients with deficit and non-deficit syndrome. Psychiatry Res. 30, 199–205.

Harvey, P.D., Howanitz, E., Parrella, M., White, L., Davidson, M., Mohs, R.C., Hoblyn, J., Davis, K.L., 1998. Symptoms, cognitive functioning, and adaptive skills in geriatric patients with lifelong schizophrenia: a comparison across treatment sites. Am. J. Psychiatry 155, 1080–1086.

Heinrichs, R.W., Zakzanis, K.K., 1998. Neurocognitive deficit in schizophrenia: a quantitative review of the evidence. Neuropsychology 12, 426–445.

Heydebrand, G., Weiser, M., Rabinowitz, J., Hoff, A.L., DeLisi, L.E., Csernansky, J.G., 2004. Correlates of cognitive deficits in first episode schizophrenia. Schizophr. Res. 68, 1–9.

Hoshi, Y., 2003. Functional near-infrared optical imaging: utility and limitation in human brain mapping. Psychophysiology 40, 511–520.

Hoshi, Y., Kobayashi, N., Tamura, M., 2001. Interpretation of near-infrared spectroscopy signals: a study with a newly developed perfused rat brain model. J. Appl. Physiol. 90, 1657–1662.

Hoshi, Y., Shinba, T., Sato, C., Doi, N., 2006. Resting hypofrontality in schizophrenia: a study using near-infrared time-resolved spectroscopy. Schizophr. Res. 84, 411–420.

Inada, T., 1996. Evaluation and Diagnosis of Drug-induced Extrapyramidal Symptoms: Commentary on the DIEPSS and Guide to its Usage. Seiwa Shoten, Tokyo.

Jobsis, F.F., 1977. Noninvasive infrared monitoring of cerebral and myocardial oxygen sufficiency and circulatory parameters. Science 198, 1264–1267.

Johnson, M.R., Morris, N.A., Astur, R.S., Calhoun, V.D., Mathalon, D.H., Kiehl, K.A., Pearlson, G.D., 2006. A functional magnetic resonance imaging study of working memory abnormalities in schizophrenia. Biol. Psychiatry 60, 11–21.

Kameyama, M., Fukuda, M., Uehara, T., Mikuni, M., 2004. Sex and age dependencies of cerebral blood volume changes during cognitive activation: a multichannel near-infrared spectroscopy study. Neuroimage 22, 1715–1721.
Kameyama, M., Fukuda, M., Yamagishi, Y., Sato, T., Uehara, T., Ito, M., Suto, T., Mikuni, M., 2006. Frontal lobe function in bipolar disorder: a multichannel near-infrared spectroscopy study. Neuroimage 29, 172–184.
Kawaguchi, S., Ukai, S., Shinosaki, K., Ishii, R., Yamamoto, M., Ogawa, A., Mizuno-Matsumoto, Y., Fujita, N., Yoshimine, T., Takeda, M., 2005. Information processing flow and neural activations in the dorsolateral prefrontal cortex in the Stroop task in schizophrenic patients. A spatially filtered MEG analysis with high temporal and spatial resolution. Neuropsychobiology 51, 191–203.
Kay, S.R., Fiszbein, A., Opler, L.A., 1987. The positive and negative syndrome scale (PANSS) for schizophrenia. Schizophr. Bull. 13, 261–276.
Keefe, R.S., Silva, S.G., Perkins, D.O., Lieberman, J.A., 1999. The effects of atypical antipsychotic drugs on neurocognitive impairment in schizophrenia: a review and meta-analysis. Schizophr. Bull. 25, 201–222.
Kerns, J.G., Cohen, J.D., MacDonald III, A.W., Johnson, M.K., Stenger, V.A., Aizenstein, H., Carter, C.S., 2005. Decreased conflict- and error-related activity in the anterior cingulate cortex in subjects with schizophrenia. Am. J. Psychiatry 162, 1833–1839.
Kleinschmidt, A., Obrig, H., Requardt, M., Merboldt, K.D., Dirnagl, U., Villringer, A., Frahm, J., 1996. Simultaneous recording of cerebral blood oxygenation changes during human brain activation by magnetic resonance imaging and near-infrared spectroscopy. J. Cereb. Blood Flow Metab. 16, 817–826.
Kubota, Y., Toichi, M., Shimizu, M., Mason, R.A., Coconcea, C.M., Findling, R.L., Yamamoto, K., Calabrese, J.R., 2005. Prefrontal activation during verbal fluency tests in schizophrenia–a near-infrared spectroscopy (NIRS) study. Schizophr. Res. 77, 65–73.
Lindenmayer, J.P., Bernstein-Hyman, R., Grochowski, S., 1994. A new five factor model of schizophrenia. Psychiatr. Q. 65, 299–322.
Ma, X., Wang, Q., Sham, P.C., Liu, X., Rabe-Hesketh, S., Sun, X., Hu, J., Meng, H., Chen, W., Chen, E.Y., Deng, W., Chan, R.C., Murray, R.M., Collier, D.A., Li, T., 2007. Neurocognitive deficits in first-episode schizophrenic patients and their first-degree relatives. Am. J. Med. Genet. B Neuropsychiatr. Genet. 144, 407–416.
Manoach, D.S., 2003. Prefrontal cortex dysfunction during working memory performance in schizophrenia: reconciling discrepant findings. Schizophr. Res. 60, 285–298.
Martin, A., Wiggs, C.L., Lalonde, F., Mack, C., 1994. Word retrieval to letter and semantic cues: a double dissociation in normal subjects using interference tasks. Neuropsychologia 32, 1487–1494.
Matsuoka, K., Uno, M., Kasai, K., Koyama, K., Kim, Y., 2006. Estimation of premorbid IQ in individuals with Alzheimer's disease using Japanese ideographic script (Kanji) compound words: Japanese version of National Adult Reading Test. Psychiatry Clin. Neurosci. 60, 332–339.
Mehagnoul-Schipper, D.J., van der Kallen, B.F., Colier, W.N., van der Sluijs, M.C., van Erning, L.J., Thijssen, H.O., Oeseburg, B., Hoefnagels, W.H., Jansen, R.W., 2002. Simultaneous measurements of cerebral oxygenation changes during brain activation by near-infrared spectroscopy and functional magnetic resonance imaging in healthy young and elderly subjects. Hum. Brain Mapp. 16, 14–23.
Morris, R.G., Miotto, E.C., Feigenbaum, J.D., 1997. Planning ability after frontal and temporal lobe lesions in humans: the effects of selection equivocation and working memory load. Cognitiveneuropsychology 14, 1007–1027.
Nakahachi, T., Ishii, R., Iwase, M., Canuet, L., Takahashi, H., Kurimoto, R., Ikezawa, K., Azechi, M., Sekiyama, R., Honaga, E., Uchiumi, C., Iwakiri, M., Motomura, N., Takeda, M., 2008. Frontal activity during the digit symbol substitution test determined by multichannel near-infrared spectroscopy. Neuropsychobiology 57, 151–158.
Nasrallah, H.A., Schwarzkopf, S.B., Olson, S.C., Coffman, J.A., 1990. Gender differences in schizophrenia on MRI brain scans. Schizophr. Bull. 16, 205–210.
Okada, F., Tokumitsu, Y., Hoshi, Y., Tamura, M., 1994. Impaired interhemispheric integration in brain oxygenation and hemodynamics in schizophrenia. Eur. Arch. Psychiatry Clin. Neurosci. 244, 17–25.
Okamoto, M., Dan, H., Sakamoto, K., Takeo, K., Shimizu, K., Kohno, S., Oda, I., Isobe, S., Suzuki, T., Kohyama, K., Dan, I., 2004. Three-dimensional probabilistic anatomical cranio-cerebral correlation via the international 10–20 system oriented for transcranial functional brain mapping. Neuroimage 21, 99–111.
Oldfield, R.C., 1971. The assessment and analysis of handedness: the Edinburgh inventory. Neuropsychologia 9, 97–113.
Pratt, J.A., Winchester, C., Egerton, A., Cochran, S.M., Morris, B.J., 2008. Modelling prefrontal cortex deficits in schizophrenia: implications for treatment. Br. J. Pharmacol. 153 (Suppl 1), S465–S470.
Ragland, J.D., Yoon, J., Minzenberg, M.J., Carter, C.S., 2007. Neuroimaging of cognitive disability in schizophrenia: search for a pathophysiological mechanism. Int. Rev. Psychiatry 19, 417–427.
Reinsel, R.A., Veselis, R.A., Dnistrian, A.M., Feshchenko, V.A., Beattie, B.J., Duff, M.R., 2000. Midazolam decreases cerebral blood flow in the left prefrontal cortex in a dose-dependent fashion. Int. J. Neuropsychopharmacol. 3, 117–127.
Richter, M.M., Herrmann, M.J., Ehlis, A.C., Plichta, M.M., Fallgatter, A.J., 2007. Brain activation in elderly people with and without dementia: influences of gender and medication. World J. Biol. Psychiatry 8, 23–29.
Schlösser, R.G., Koch, K., Wagner, G., Nenadic, I., Roebel, M., Schachtzabel, C., Axer, M., Schultz, C., Reichenbach, J.R., Sauer, H., 2008. Inefficient executive cognitive control in schizophrenia is preceded by altered functional activation during information encoding: an fMRI study. Neuropsychologia 46, 336–347.
Semkovska, M., Bédard, M.A., Stip, E., 2001. Hypofrontality and negative symptoms in schizophrenia: synthesis of anatomic and neuropsychological knowledge and ecological perspectives. Encephale 27, 405–415.
Shinba, T., Nagano, M., Kariya, N., Ogawa, K., Shinozaki, T., Shimosato, S., Hoshi, Y., 2004. Near-infrared spectroscopy analysis of frontal lobe dysfunction in schizophrenia. Biol. Psychiatry 55, 154–164.
Soul, J.S., du Plessis, A.J., 1999. New technologies in pediatric neurology. Near-infrared spectroscopy. Semin. Pediatr. Neurol. 6, 101–110.
Sternberg, S., 1966. High-speed scanning in human memory. Science 153, 652–654.
Strangman, G., Culver, J.P., Thompso, J.H., Boas, D.A., 2002. A quantitative comparison of simultaneous BOLD fMRI and NIRS recordings during functional brain activation. Neuroimage 17, 719–731.
Suto, T., Fukuda, M., Ito, M., Uehara, T., Mikuni, M., 2004. Multichannel near-infrared spectroscopy in depression and schizophrenia: cognitive brain activation study. Biol. Psychiatry 55, 501–511.
Takizawa, R., Kasai, K., Kawakubo, Y., Marumo, K., Kawasaki, S., Yamasue, H., Fukuda, M., 2008. Reduced frontopolar activation during verbal fluency task in schizophrenia: a multi-channel near-infrared spectroscopy study. Schizophr. Res. 99, 250–262.
Toronov, V., Webb, A., Choi, J.H., Wolf, M., Michalos, A., Gratton, E., Hueber, D., 2001. Investigation of human brain hemodynamics by simultaneous near-infrared spectroscopy and functional magnetic resonance imaging. Med. Phys. 28, 521–527.
Watanabe, A., Kato, T., 2004. Cerebrovascular response to cognitive tasks in patients with schizophrenia measured by near-infrared spectroscopy. Schizophr. Bull. 30, 435–444.
Yamamoto, T., Kato, T., 2002. Paradoxical correlation between signal in functional magnetic resonance imaging and deoxygenated haemoglobin content in capillaries: a new theoretical explanation. Phys. Med. Biol. 47, 1121–1141.

Biochemical and Biophysical Research Communications 379 (2009) 191–195

Contents lists available at ScienceDirect

Biochemical and Biophysical Research Communications

journal homepage: www.elsevier.com/locate/ybbrc

Dysbindin engages in c-Jun N-terminal kinase activity and cytoskeletal organization

Kyoko Kubota [a,1], Natsuko Kumamoto [a,1], Shinsuke Matsuzaki [a,b,*], Ryota Hashimoto [b,c,d], Tsuyoshi Hattori [a,b,g], Hiroaki Okuda [a,e], Hironori Takamura [c,d], Masatoshi Takeda [b,c], Taiichi Katayama [f], Masaya Tohyama [a,b]

[a] Department of Anatomy and Neuroscience, Osaka University Graduate School of Medicine, Suita, Osaka, Japan
[b] The Osaka-Hamamatsu Joint Research Center for Child Mental Development, Osaka University Graduate School of Medicine, Suita, Osaka, Japan
[c] Department of Psychiatry, Osaka University Graduate School of Medicine, Suita, Osaka, Japan
[d] CREST (Core Research for Evolutionary Science and Technology), JST (Japan Science and Technology Agency), Kawaguchi, Saitama, Japan
[e] Department of Anatomy and Neuroscience, Faculty of Medicine, Nara Medical University, Kashihara, Nara, Japan
[f] Department of Anatomy and Neuroscience, Hamamatsu University School of Medicine, Hamamatsu, Shizuoka, Japan
[g] Department of Molecular Neuropsychiatry, Osaka University Graduate School of Medicine, Suita, Osaka, Japan

ARTICLE INFO

Article history:
Received 2 December 2008
Available online 16 December 2008

Keywords:
Dysbindin
Schizophrenia
c-Jun N-terminal kinase
Actin cytoskeleton

ABSTRACT

A number of reports have provided genetic evidence for an association between the DTNBP1 gene (coding dysbindin) and schizophrenia. In addition, sandy mice, which harbor a deletion in the DTNBP1 gene and lack dysbindin, display behavioral abnormalities suggestive of an association with schizophrenia. However, the mechanism by which the loss of dysbindin induces schizophrenia-like behaviors remains unclear. Here, we report that small interfering RNA-mediated knockdown of dysbindin resulted in the aberrant organization of actin cytoskeleton in SH-SY5Y cells. Furthermore, we show that morphological abnormalities of the actin cytoskeleton were similarly observed in growth cones of cultured hippocampal neurons derived from sandy mice. Moreover, we report a significant correlation between dysbindin expression level and the phosphorylation level of c-Jun N-terminal kinase (JNK), which is implicated in the regulation of cytoskeletal organization. These findings suggest that dysbindin plays a key role in coordinating JNK signaling and actin cytoskeleton required for neural development.

Schizophrenia is a heritable mental disease that devastates about 1% of the population worldwide, affecting their perception, emotion, and judgment [1]. The DTNBP1 gene (coding dysbindin: dystrobrevin binding protein (1) was identified as a candidate for involvement in schizophrenia [2]. In studies of postmortem brain tissue, patients with schizophrenia had lower dysbindin expression than controls [3–5]. Moreover, long-term treatment with typical or atypical antipsychotics did not alter the mRNA expression levels or protein levels of dysbindin in the mouse frontal cortex and hippocampus [4,6]. Together these findings suggest that decreased dysbindin levels may confer susceptibility to schizophrenia. Sandy (*sdy*) mice that express no dysbindin, owing to a deletion of the DTNBP1 gene showed behavioral abnormalities such as reduced activity, heightened anxiety-like response, and deficits in social interaction, memory, and learning [7–9], which could be endophenotypes of schizophrenia. *sdy* mice also displayed lower levels of dopamine, but not glutamate, in the cerebral cortex, hippocampus, and hypothalamus [8,10].

Dysbindin is known to be widely distributed in the brain and located presynaptically and postsynaptically in the central nervous system [11]. The downregulation of endogenous dysbindin by small interfering RNA (siRNA) reportedly inhibited the release of glutamate from hippocampal cultured neurons and increased the release of dopamine from PC12 cells [12,13]. In addition, *sdy* mice reportedly exhibit defective synaptic structure and function in the hippocampal CA1 neurons [14]. However, the molecular mechanism underlying the effects of dysbindin on synaptogenesis remains elusive. On the other hand, an increasing number of studies have shown that cytoskeletal organization is essential for the dynamics of synaptogenesis [15,16]. Therefore, to examine the effects of low dysbindin levels on cytoskeletal organization, we performed an immunocytochemical analysis using SH-SY5Y cells, which have been used as an *in vitro* model to study neural development. Furthermore, to confirm the influences of dysbindin knockdown *in vivo*, we analyzed *sdy* mice similarly. In addition, we investigated whether alterations in dysbindin expression affect c-Jun N-terminal kinase (JNK) activity, which has been known to phosphorylate many cytoskeletal proteins and regulate neural development [17–20].

* Corresponding author. Address: Department of Anatomy and Neuroscience, Osaka University Graduate School of Medicine, Suita, Osaka, Japan. Fax: +81 6 6879 3229.
E-mail address: s-matsuzaki@anat2.med.osaka-u.ac.jp (S. Matsuzaki).
[1] Joint first authors.

0006-291X/$ - see front matter © 2008 Elsevier Inc. All rights reserved.
doi:10.1016/j.bbrc.2008.12.017

Materials and methods

Mice. The *sdy* and control DBA/2J mice were originally obtained from the Jackson Laboratory and bred in the Institute of Experimental Animal Sciences, Osaka University Graduate School of Medicine. All the experiments were performed in accordance with our institutional guidelines after obtaining the permission of the Laboratory Animal Committee.

Cell culture. The SH-SY5Y cell line was obtained from the European Collection of Cell Culture (Wiltshire, UK) and maintained according to the manufacturer's protocol. Hippocampal neurons were cultured from E15 mice embryos using the Nerve-cell Culture System (SUMITOMO BAKELITE, Tokyo, Japan). Neurons (2.1×10^5) in MEM (Invitrogen) containing 10% fetal horse serum and antibiotics (50 U/ml penicillin G and 50 μg/ml streptomycin) were plated onto 3.5 cm poly-L-lysine-coated dish. After 4 h of incubation, medium was changed to Neurobasal Medium containing 2% B27 (Invitrogen) and antibiotics.

Plasmid. FLAG-human *dysbindin* (AF394226) was cloned into pcDNA 3.1/Zeo (+) vector (Invitrogen). Transfection into cells was performed with Lipofectamine 2000 (Invitrogen) according to the manufacturer's protocol.

RNA interference. We used 5′-AAGUGACAAGUCAAGAGAA-3′ siRNA, the sequence of which is corresponding to nucleotides 175–197 of human dysbindin mRNA. Scrambled siRNA 5′-UUCUCUUGACUUGUCACUU-3′ was used as a negative control. Both sense and antisense strands with two base overhangs were synthesized by NIPPON-EGT (Toyama, Japan) in desalted form. siRNA transfection was performed with Lipofectamine RNAiMAX (Invitrogen) according to the manufacturer's protocol.

Immunocytochemistry. Plasmid-transfected cells were fixed with cold 95% ethanol for 7 min at −20 °C and subjected to blocking in 2% BSA/PBS for 10 min. After incubating with an anti-FLAG antibody (1:150, Sigma–Aldrich, St. Louis, USA) overnight, cells were incubated with an Alexa 488 conjugated anti-rabbit secondary antibody (1:500, Invitrogen) for 2 h. siRNA-transfected cells were fixed with cold methanol for 10 min at −20 °C and incubated in PBS containing 5% BSA and 0.3% Triton X-100 for 30 min. The cells were then incubated with an anti-β-tubulin antibody (1:500, Sigma–Aldrich) at 4 °C overnight followed by an Alexa 568 conjugated anti-mouse secondary antibody (1:500, Invitrogen) for 2 h. For detection of actin filament, cells were fixed with 2.5% paraformaldehyde/PBS for 20 min, subjected to permeabilization with 0.1% Triton X-100/PBS for 3 min and then incubated with the Alexa Fluor 568 phalloidin staining solution (5 U/ml, Invitrogen) in PBS containing 1% BSA for 20 min. The coverslips were mounted onto the slides using VECTASHIELD Mounting Medium with DAPI (Vector Laboratories, Peterborough, England). Fluorescence images were acquired using a digital camera DP70 connected with a stereomicroscope (Carl Zeiss, Oberkochen, Germany). Hippocampal cultured neurons at stage 3 were similarly subjected to immunocytochemistry. Fluorescence images were acquired using a confocal laser scanning microscope (LSM-510 UV/META, Carl Zeiss).

Western blot analysis. siRNA-transfected cells were lysed in RIPA buffer containing 1 mM Na_3VO_4, 1 mM NaF and Protease Inhibitor Cocktail (Roche Diagnostics, Basel, Switzerland), incubated for 20 min at 4 °C and centrifuged at 17,000*g* for 20 min at 4 °C. Proteins (3 μg) were separated on SDS–PAGE and electrotransferred onto Immobilon-P Transfer Membranes (MILLIPORE, Billerica, USA). Membranes were incubated in PBS containing 5% skim milk and 0.05% Tween 20 for 1 h and blotted with primary antibodies at 4 °C overnight. An anti-dysbindin antibody (1:1000), anti-phospho-JNK antibody (1:1000, Cell Signaling Technology, Danvers, USA), anti-JNK antibody (1:1000, Cell Signaling Technology) and anti-GAPDH antibody (1:5000, Abcam, Cambridge, USA) were used as primary antibodies. The membranes were incubated with an anti-mouse or anti-rabbit HRP-linked secondary antibody (1:2000, Cell Signaling Technology) for 1 h. Mouse monoclonal anti-dysbindin antibody was produced using the GST fused human dysbindin as antigen. High titer clones to dysbindin were selected by ELISA using the dysbindin protein and the immunoreactivity of the clones were checked by Western blot analysis. For analyses of mice, hemisphere of E16 embryo was homogenized in RIPA buffer and similarly subjected to Western blot analysis.

Results

Portions of dysbindin were localized to the tips of protrusions, and dysbindin knockdown influenced the organization of actin cytoskeleton in SH-SY5Y cells

Dysbindin was previously shown to exist in axon terminals in the hippocampus and to decline in patients with schizophrenia [4,11]. However, dysbindin's function in axon terminals in the hippocampus remains unclear. Thus, to explore the role of dysbindin in neurite formation, we attempted to downregulate it in differentiating SH-SY5Y cells. To clarify how dysbindin operates at the tip of a protrusion, we used an RNA interference method to investigate whether or not alterations in dysbindin expression could influence the morphology of the terminal region of protrusions. Retinoic acid treatment gives rise to the differentiation of SH-SY5Y cells and induces neurite outgrowth [21,22]. Control or dysbindin siRNA-transfected SH-SY5Y cells were incubated with retinoic acid to differentiate and then were analyzed in cytoskeletal organization by visualizing actin filament with rhodamine-phalloidin. Interestingly, the organization of actin cytoskeleton at the tips of neurites of differentiating SH-SY5Y cells was dramatically disrupted by the dysbindin knockdown (Fig. 1A). In addition, immunocytochemical analysis with anti-β-tubulin antibody was performed to compare the lengths of neurites of dysbindin knockdown cells to those of controls. As shown in Fig. 1B, the β-tubulin-positive neurites of dysbindin knockdown cells were apparently shorter than those of the controls. We confirmed that dysbindin with FLAG-tag was expressed in the cell body as well as at the tips of protrusions of SH-SY5Y cells (Fig. 1C). These results suggest that dysbindin knockdown significantly affects the organization of actin cytoskeleton, bringing about the inhibition of neurite outgrowth in differentiating SH-SY5Y cells.

The derangement of cytoskeletal organization was observed in growth cones of hippocampal cultured neurons derived from sdy mice

To confirm the effects of dysbindin knockdown on actin cytoskeleton, we analyzed hippocampal cultured neurons derived from *sdy* mice, which lack dysbindin. The growth cone consists mainly of actin-based structures and can be divided into three distinct regions: the peripheral domain, the central domain, and the transition zone [15]. The peripheral domain has linear actin bundles comprising filopodia and mesh-like gels comprising lamellipodia. The central domain, which is rich in microtubules, has hardly any actin superstructures. In the transition zone located between the peripheral domain and the central domain, transverse bundles of actin filaments are observed. To explore the effects of dysbindin knockdown on actin cytoskeleton in growth cones, hippocampal neurons prepared from E15 mice embryos were cultured, fixed at stage 3, and stained with rhodamine-phalloidin. In neurons derived from wild-type mice, most of the growth cones had a characteristic shape (Fig. 2A). In contrast, the growth cones of neurons derived from *sdy* mice showed significant changes in actin-based

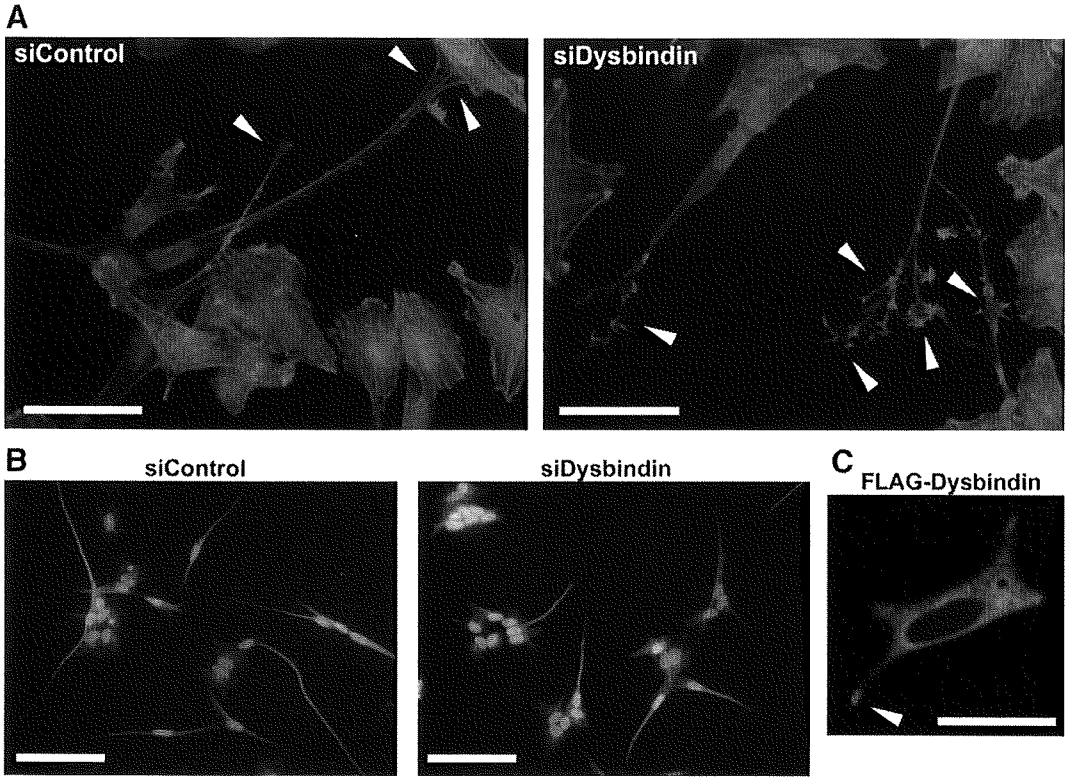

Fig. 1. Dysbindin is involved in neurite morphogenesis. (A) The effects of dysbindin knockdown on actin cytoskeleton. SH-SY5Y cells were transfected with control (siControl) or dysbindin siRNA (siDysbindin), followed by incubation with retinoic acid for 60 h. Actin filament was visualized by rhodamine-phalloidin (red) and DAPI (blue). Bar = 50 μm. (B) The effects of dysbindin knockdown on neurite length. SH-SY5Y cells were transfected with control (siControl) or dysbindin (siDysbindin) siRNA, followed by incubation with retinoic acid for 60 h. The cells were then immunostained using anti-β-tubulin antibody (red) followed by Alexa 568-labeled secondary antibody and DAPI (blue). Bar = 100 μm. (C) Localization of dysbindin in cell body and at the tips of protrusions. SH-SY5Y cells were transfected with FLAG-tagged dysbindin. They were cultured for 24 h and stained with anti-FLAG antibody, followed by Alexa 488-labeled secondary antibody. Bar = 25 μm. (For interpretation of color mentioned in this figure the reader is referred to the web version of the article.)

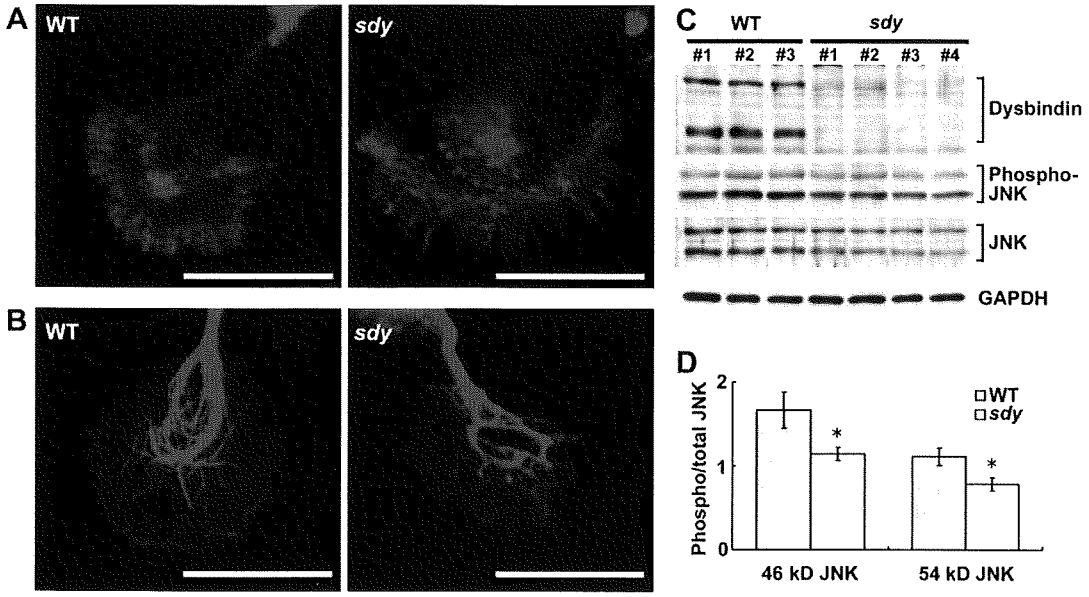

Fig. 2. Dysbindin is involved in the regulation of growth cone morphology. (A) Actin cytoskeleton within the growth cone. Embryonic hippocampi were dissociated from E15 wild-type (WT) or *sdy* mice (*sdy*) and cultured. They were stained with rhodamine-phalloidin to visualize actin filament at stage 3. Bar = 20 μm. (B) Microtubule cytoskeleton within the growth cone. Embryonic hippocampal neurons derived from E15 wild-type (WT) or *sdy* mice (*sdy*) were cultured. The neurons were stained with anti-β-tubulin antibody at stage 3, followed by Alexa 568-labeled secondary antibody. Bar = 20 μm. (C) JNK activity in the brains of wild-type (WT) or *sdy* mice (*sdy*). Lysates homogenized from the hemisphere of E16 embryos were immunoblotted with anti-dysbindin antibody, anti-phosphorylated JNK antibody, anti-JNK antibody, and anti-GAPDH antibody. (D) Quantitated data. Relative ratios of 46 kDa phospho/total JNK and 54 kDa phospho/total JNK in the brains of wild-type (WT) or *sdy* mice (*sdy*) were analyzed using NIH ImageJ software and represented graphically. Statistical comparisons were performed using the unpaired Student's *t*-test. Data represent means ± SD. $^{*}P < 0.05$ versus control.

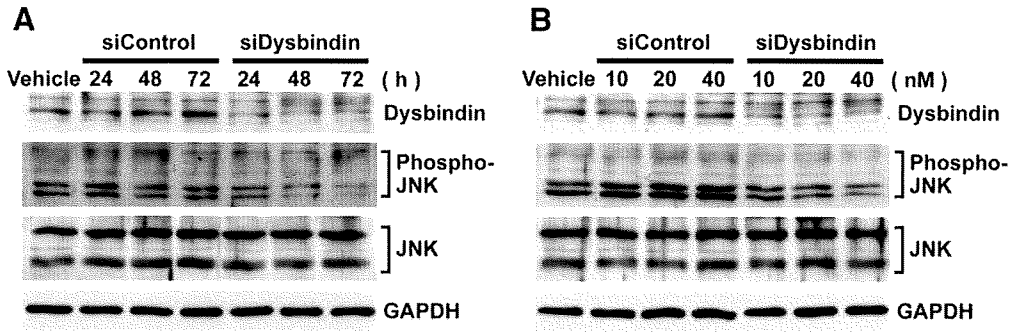

Fig. 3. The JNK phosphorylation level was susceptible to the dysbindin expression level. (A) Time-course dependent effects of dysbindin siRNA on the expression level of dysbindin and phosphorylated JNK. SH-SY5Y cells were transfected with control (siControl) or dysbindin siRNA (siDysbindin), incubated for the indicated times, and subjected to immunoblotting with anti-dysbindin antibody, anti-phosphorylated JNK antibody, anti-JNK antibody, and anti-GAPDH antibody. (B) Dose-dependent effects of dysbindin siRNA on the dysbindin and phosphorylated JNK expression levels. SH-SY5Y cells were transfected with the indicated volumes of control (siControl) or dysbindin siRNA (siDysbindin) for 48 h and harvested. Lysates were immunoblotted with anti-dysbindin antibody, anti-phosphorylated JNK antibody, anti-JNK antibody, and anti-GAPDH antibody.

structures. In those neurons, transverse bundles of actin filament in the transition zone disappeared, and then the central domain became difficult to discern. Additionally, in the peripheral domain, the palm-like shapes consisting of filopodia and lamellipodia were perturbed. On the other hand, microtubules are known to organize into bundles in the neurites, whereas upon entering the central domain of growth cones, they diverge from each other and collaborate with the actin cytoskeleton to contribute growth cone motility and axon elongation [23]. Then, we analyzed microtubule stabilization by staining β-tubulin with a specific antibody. The results revealed that microtubules in the growth cones of neurons derived from *sdy* mice were affected slightly, whereas the controls were unaffected (Fig. 2B). Our findings suggest that hippocampal neurons in *sdy* mice may tend to show the morphological disorder of growth cones.

JNK activity was suggested to be attenuated in the brains of sdy mice embryos

Recent works have shown that activated JNK might play a role in axon formation [20,24]. In hippocampal cultured neurons, JNK has been known to be predominately distributed with cytoskeleton-associated structures such as growth cones [25]. Interestingly, we previously performed pathway analysis with the dysbindin binding proteins, interactions of which were detected by yeast two-hybrid screening, and then found that JNK signaling is a candidate pathway for involvement in dysbindin function (personal communication). Thus, to examine whether or not JNK activity could be altered in the brains of *sdy* mice compared to those of the wild type, a hemisphere from each of seven E16 embryos was homogenized in lysis buffer and subjected to Western blotting analysis. As previously reported [7], we confirmed that the expression of both 50 kDa and 40 kDa dysbindin are abolished in *sdy* mice. Intriguingly, the phosphorylated JNK was lower in the brain lysate derived from *sdy* mice compared to that from the wild type, indicating that dysbindin might regulate the organization of actin cytoskeleton via modulating JNK activity (Fig. 2C and D).

The phosphorylation level of JNK was reduced in proportion with the dysbindin expression level in SH-SY5Y cells

To determine whether or not a reduction in JNK activity was due specifically to the loss of dysbindin, we compared the JNK phosphorylation level with the dysbindin expression level in control or dysbindin siRNA-treated SH-SY5Y cells by Western blot analysis. Though two splice variants of dysbindin exist in DBA/2J mice (Fig. 2C), SH-SY5Y cells predominantly express 50 kDa dysbindin in our experiments. The downregulation of dysbindin was observed in a time-dependent manner in dysbindin siRNA-treated cells, and then phosphorylated JNK was similarly decreased in proportion to the dysbindin expression level (Fig. 3A). In addition, we performed dose–response analysis with each siRNA and found that the expression level of phosphorylated JNK is highly sensitive to that of dysbindin (Fig. 3B). Our data unequivocally demonstrate that there is a significant correlation between dysbindin level and JNK activity.

Discussion

Recent studies have suggested that dysfunction in neurodevelopment and neurotransmission is important for the etiology of schizophrenia [26,27]. For example, DISC1, a candidate gene for susceptibility to schizophrenia, has been known to be part of the NUDEL/LIS1/14-3-3ε complex and to regulate the transport of the protein complex into axons, leading to neuronal migration and axon elongation [28,29]. On the other hand, it has been reported that dysbindin might influence the exocytotic glutamate release and the dopaminergic system via modulation of SNAP25 and synapsin 1 expression [12,13]. Additionally, dysbindin has been suggested to regulate cell surface levels of DRD2 (dopamine D2 receptor) and the strength of the DRD2-mediated G_i signaling pathway [30]. Although a common molecular mechanism under these observations has long been unexplained, morphological abnormalities in developing neurons, which may bring about subsequent dysfunction of synapses, shall be one of the probable causes of susceptibility to schizophrenia.

In this study, we show that dysbindin is required for the normal arrangement of actin cytoskeleton, especially at neurite tips, in differentiating SH-SY5Y cells. Furthermore, we found that the morphological abnormalities are observed in growth cones of cultured hippocampal neurons derived from *sdy* mice, which lack dysbindin. In developing neurons, growth cones are involved in axon elongation and migration [31]. Therefore, the morphological dysfunction of growth cones by a loss of dysbindin may result in an insufficiency of neural circuit formation and synaptogenesis.

Recently, an increasing number of reports have strongly suggested that JNK is relevant to cytoskeletal function [25]. Moreover, it has been demonstrated that phosphorylated JNK was enriched in axons and necessary for proper axon development [20,25]. The JNK family consists of three isoforms: JNK1, JNK2, and JNK3 [32]. Mice devoid of both JNK1 and JNK2 suffer from multiple abnormalities during development of the central nervous system [33]. In addi-

tion, the mutation of JNK3 gene reportedly results in the severe encephalopathy phenotype in children [34]. Interestingly, the present study revealed that the phosphorylation level of JNK is altered by the expression level of dysbindin, raising the possibility that dysbindin functions as a mediator of the JNK signaling pathway, at least at neurite ends, where dysbindin is colocalized with JNK.

Hence, we speculate that a loss of dysbindin results in the failure of normal axon guidance by the disruption of growth cones during the embryonic stage and evokes aberrations in the neurosecretory system in adulthood. However, it remains unclear how dysbindin regulates JNK phosphorylation and how the morphological changes of growth cones in developing neurons contribute to the pathogenic mechanism of schizophrenia. Further analyses are needed to obtain the precise molecular function of dysbindin.

Acknowledgments

This work was in part supported by the 21st Century COE program and by the Osaka Medical Research Foundation for Incurable Diseases. We appreciate Etsuko Moriya and Yoko Ohashi preparing for our experiments.

References

[1] R. Freedman, Schizophrenia, N. Engl. J. Med. 349 (2003) 1738–1749.
[2] R.E. Straub, Y. Jiang, C.J. MacLean, Y. Ma, B.T. Webb, M.V. Myakishev, C. Harris-Kerr, B. Wormley, H. Sadek, B. Kadambi, A.J. Cesare, A. Gibberman, X. Wang, F.A. O'Neill, D. Walsh, K.S. Kendler, Genetic variation in the 6p22.3 gene DTNBP1, the human ortholog of the mouse dysbindin gene, is associated with schizophrenia, Am. J. Hum. Genet. 71 (2002) 337–348.
[3] N.J. Bray, A. Preece, N.M. Williams, V. Moskvina, P.R. Buckland, M.J. Owen, M.C. O'Donovan, Haplotypes at the dystrobrevin binding protein 1 (DTNBP1) gene locus mediate risk for schizophrenia through reduced DTNBP1 expression, Hum. Mol. Genet. 14 (2005) 1947–1954.
[4] K. Talbot, W.L. Eidem, C.L. Tinsley, M.A. Benson, E.W. Thompson, R.J. Smith, C.G. Hahn, S.J. Siegel, J.Q. Trojanowski, R.E. Gur, D.J. Blake, S.E. Arnold, Dysbindin-1 is reduced in intrinsic, glutamatergic terminals of the hippocampal formation in schizophrenia, J. Clin. Invest. 113 (2004) 1353–1363.
[5] C.S. Weickert, R.E. Straub, B.W. McClintock, M. Matsumoto, R. Hashimoto, T.M. Hyde, M.M. Herman, D.R. Weinberger, J.E. Kleinman, Human dysbindin (DTNBP1) gene expression in normal brain and in schizophrenic prefrontal cortex and midbrain, Arch. Gen. Psychiatry 61 (2004) 544–555.
[6] S. Chiba, R. Hashimoto, S. Hattori, M. Yohda, B. Lipska, D.R. Weinberger, H. Kunugi, Effect of antipsychotic drugs on DISC1 and dysbindin expression in mouse frontal cortex and hippocampus, J. Neural Transm. 113 (2006) 1337–1346.
[7] Y.Q. Feng, Z.Y. Zhou, X. He, H. Wang, X.L. Guo, C.J. Hao, Y. Guo, X.C. Zhen, W. Li, Dysbindin deficiency in sandy mice causes reduction of snapin and displays behaviors related to schizophrenia, Schizophr. Res. 106 (2008) 218–228.
[8] S. Hattori, T. Murotani, S. Matsuzaki, T. Ishizuka, N. Kumamoto, M. Takeda, M. Tohyama, A. Yamatodani, H. Kunugi, R. Hashimoto, Behavioral abnormalities and dopamine reductions in sdy mutant mice with a deletion in Dtnbp1, a susceptibility gene for schizophrenia, Biochem. Biophys. Res. Commun. 373 (2008) 298–302.
[9] K. Takao, K. Toyama, K. Nakanishi, S. Hattori, H. Takamura, M. Takeda, T. Miyakawa, R. Hashimoto, Impaired long-term memory retention and working memory in sdy mutant mice with a deletion in Dtnbp1, a susceptibility gene for schizophrenia, Mol. Brain 1 (2008) 11.
[10] T. Murotani, T. Ishizuka, S. Hattori, R. Hashimoto, S. Matsuzaki, A. Yamatodani, High dopamine turnover in the brains of Sandy mice, Neurosci. Lett. 421 (2007) 47–51.
[11] M.A. Benson, S.E. Newey, E. Martin-Rendon, R. Hawkes, D.J. Blake, Dysbindin, a novel coiled-coil-containing protein that interacts with the dystrobrevins in muscle and brain, J. Biol. Chem. 276 (2001) 24232–24241.
[12] N. Kumamoto, S. Matsuzaki, K. Inoue, T. Hattori, S. Shimizu, R. Hashimoto, A. Yamatodani, T. Katayama, M. Tohyama, Hyperactivation of midbrain dopaminergic system in schizophrenia could be attributed to the down-regulation of dysbindin, Biochem. Biophys. Res. Commun. 345 (2006) 904–909.
[13] T. Numakawa, Y. Yagasaki, T. Ishimoto, T. Okada, T. Suzuki, N. Iwata, N. Ozaki, T. Taguchi, M. Tatsumi, K. Kamijima, R.E. Straub, D.R. Weinberger, H. Kunugi, R. Hashimoto, Evidence of novel neuronal functions of dysbindin, a susceptibility gene for schizophrenia, Hum. Mol. Genet. 13 (2004) 2699–2708.
[14] X.W. Chen, Y.Q. Feng, C.J. Hao, X.L. Guo, X. He, Z.Y. Zhou, N. Guo, H.P. Huang, W. Xiong, H. Zheng, P.L. Zuo, C.X. Zhang, W. Li, Z. Zhou, DTNBP1, a schizophrenia susceptibility gene, affects kinetics of transmitter release, J. Cell Biol. 181 (2008) 791–801.
[15] C.W. Pak, K.C. Flynn, J.R. Bamburg, Actin-binding proteins take the reins in growth cones, Nat. Rev. Neurosci. 9 (2008) 136–147.
[16] Y. Sekino, N. Kojima, T. Shirao, Role of actin cytoskeleton in dendritic spine morphogenesis, Neurochem. Int. 51 (2007) 92–104.
[17] B. Bjorkblom, N. Ostman, V. Hongisto, V. Komarovski, J.J. Filen, T.A. Nyman, T. Kallunki, M.J. Courtney, E.T. Coffey, Constitutively active cytoplasmic c-Jun N-terminal kinase 1 is a dominant regulator of dendritic architecture: role of microtubule-associated protein 2 as an effector, J. Neurosci. 25 (2005) 6350–6361.
[18] L. Chang, Y. Jones, M.H. Ellisman, L.S. Goldstein, M. Karin, JNK1 is required for maintenance of neuronal microtubules and controls phosphorylation of microtubule-associated proteins, Dev. Cell 4 (2003) 521–533.
[19] A. Gdalyahu, I. Ghosh, T. Levy, T. Sapir, S. Sapoznik, Y. Fishler, D. Azoulai, O. Reiner, DCX, a new mediator of the JNK pathway, EMBO J. 23 (2004) 823–832.
[20] A.A. Oliva Jr., C.M. Atkins, L. Copenagle, G.A. Banker, Activated c-Jun N-terminal kinase is required for axon formation, J. Neurosci. 26 (2006) 9462–9470.
[21] S. Pahlman, J.C. Hoehner, E. Nanberg, F. Hedborg, S. Fagerstrom, C. Gestblom, I. Johansson, U. Larsson, E. Lavenius, E. Ortoft, et al., Differentiation and survival influences of growth factors in human neuroblastoma, Eur. J. Cancer A 31 (1995) 453–458.
[22] N. Sidell, Retinoic acid-induced growth inhibition and morphologic differentiation of human neuroblastoma cells in vitro, J. Natl. Cancer Inst. 68 (1982) 589–596.
[23] P.R. Gordon-Weeks, Organization of microtubules in axonal growth cones: a role for microtubule-associated protein MAP 1B, J. Neurocytol. 22 (1993) 717–725.
[24] S. Hirai, F. Cui de, T. Miyata, M. Ogawa, H. Kiyonari, Y. Suda, S. Aizawa, Y. Banba, S. Ohno, The c-Jun N-terminal kinase activator dual leucine zipper kinase regulates axon growth and neuronal migration in the developing cerebral cortex, J. Neurosci. 26 (2006) 11992–12002.
[25] M. Gelderblom, S. Eminel, T. Herdegen, V. Waetzig, c-Jun N-terminal kinases (JNKs) and the cytoskeleton-functions beyond neurodegeneration, Int. J. Dev. Neurosci. 22 (2004) 559–564.
[26] A. Bellon, New genes associated with schizophrenia in neurite formation: a review of cell culture experiments, Mol. Psychiatry 12 (2007) 620–629.
[27] C.A. Ross, R.L. Margolis, S.A. Reading, M. Pletnikov, J.T. Coyle, Neurobiology of schizophrenia, Neuron 52 (2006) 139–153.
[28] T. Shinoda, S. Taya, D. Tsuboi, T. Hikita, R. Matsuzawa, S. Kuroda, A. Iwamatsu, K. Kaibuchi, DISC1 regulates neurotrophin-induced axon elongation via interaction with Grb2, J. Neurosci. 27 (2007) 4–14.
[29] S. Taya, T. Shinoda, D. Tsuboi, J. Asaki, K. Nagai, T. Hikita, S. Kuroda, K. Kuroda, M. Shimizu, S. Hirotsune, A. Iwamatsu, K. Kaibuchi, DISC1 regulates the transport of the NUDEL/LIS1/14-3-3epsilon complex through kinesin-1, J. Neurosci. 27 (2007) 15–26.
[30] Y. Iizuka, Y. Sei, D.R. Weinberger, R.E. Straub, Evidence that the BLOC-1 protein dysbindin modulates dopamine D2 receptor internalization and signaling but not D1 internalization, J. Neurosci. 27 (2007) 12390–12395.
[31] J.L. Goldberg, How does an axon grow?, Genes Dev 17 (2003) 941–958.
[32] S. Gupta, T. Barrett, A.J. Whitmarsh, J. Cavanagh, H.K. Sluss, B. Derijard, R.J. Davis, Selective interaction of JNK protein kinase isoforms with transcription factors, EMBO J. 15 (1996) 2760–2770.
[33] K. Sabapathy, W. Jochum, K. Hochedlinger, L. Chang, M. Karin, E.F. Wagner, Defective neural tube morphogenesis and altered apoptosis in the absence of both JNK1 and JNK2, Mech. Dev. 89 (1999) 115–124.
[34] S.A. Shoichet, L. Duprez, O. Hagens, V. Waetzig, C. Menzel, T. Herdegen, S. Schweiger, B. Dan, E. Vamos, H.H. Ropers, V.M. Kalscheuer, Truncation of the CNS-expressed JNK3 in a patient with a severe developmental epileptic encephalopathy, Hum. Genet. 118 (2006) 559–567.

Major depression: what caused the crisis?

Nagahisa Okamoto, Yoshihiko Furusawa, Kota Sakamoto, Toshiyuki Yamamoto, Yoshiyuki Kondo, Yuko Nagafusa, Teruhiko Higuchi

Lancet 2010; 375: 346

Department of Psychiatry (N Okamoto MD, K Sakamoto MD, Y Nagafusa, T Higuchi MD), **Department of Neurology** (Y Furusawa MD, T Yamamoto MD, Y Kondo MD), **National Center Hospital of Neurology and Psychiatry, 4-1-1, Ogawahigashi, Kodaira City, Tokyo, Japan**

Correspondence to: Dr Nagahisa Okamoto, Department of Psychiatry, National Center Hospital of Neurology and Psychiatry, 4-1-1, Ogawahigashi, Kodaira City, Tokyo, 187-8551, Japan
okamoton@ncnp.go.jp

In July, 2008, a 67-year-old woman with refractory depression was referred to our institute. In 2006, she had a thymectomy for thymoma. In January, 2008, after experiencing family discord, she lost her appetite, and her bodyweight decreased by 5 kg in 1 month. She became pessimistic and self-recriminating and made several suicide attempts. CT showed no evidence of a recurrence of the thymoma. Neurological examination showed only slight muscle weakness of her limbs, but the cause of her anorexia remained unclear despite further in-hospital examinations such as gastrointestinal tract endoscopies and systemic contrast-enhanced CT. She was diagnosed as having depression and was transferred to a regional psychiatric hospital, where she was treated sequentially with sertraline, paroxetine, clomipramine, and nortriptyline, and augmentation lithium. These treatments were ineffective, and her body weight decreased from 60 kg to 33·5 kg. She was then transferred to us.

Her depressed mood, decreased interests, hypogeusia, anorexia, insomnia, anxious restlessness, decreased energy and fatigue, guilty feelings, poor concentration, and suicidal ideation persisted. She fulfilled the DSM-IV diagnostic criteria for major depressive disorder. Her total score on the 17-item Hamilton Depression Rating Scale (total-HDRS) was 40. She could walk and had no ocular and bulbar symptoms, but neurological examinations showed mild proximal muscle weakness and atrophy of her limbs. Blood test results indicated hypoalbuminaemia (albumin 3·4 g/dL); other investigations including CT chest, tumour markers, electroencephalography, and brain MRI were normal. Ten sessions of electroconvulsive therapy (ECT) were done in September, but the depressive symptoms persisted. She stopped taking medication, other than quetiapine as required (prescribed by us), but at the end of October, she suddenly developed impaired consciousness with a reduced respiratory rate. A blood gas analysis showed carbon dioxide narcosis, and she was immediately placed on a ventilator. No evidence of pulmonary disease was found, and a diagnosis of myasthenic crisis was made on the basis of a high acetylcholine receptor antibody (AchR-Ab) titre (120 nmol/L), waning on the Harvey-Masland test, and a history of thymoma. She was treated with plasmapheresis and immunoadsorption followed by prednisolone treatment (maximum dose, 50 mg/day). Her respiratory function subsequently improved, and she was extubated. In December, she was treated with pyridostigmine (180 mg/day). As the anti-AchR-Ab titre decreased, total-HDRS score improved substantially without antidepressant therapy (figure). Her long-lasting depressive symptoms improved completely, and her bodyweight recovered to 40 kg; she was discharged in July, 2009. When last seen in September, 2009, both her depression and myasthenia gravis were in remission.

The pathology of depressive symptoms associated with myasthenia gravis, including the hypothalamo-pituitary-adrenal axis dysfunction resulting from chronic stress and central cholinergic deficit, is controversial and remains to be elucidated.[1] Although some patients with major depressive disorder complicated with myasthenia gravis improve after ECT,[2] the potential to misdiagnose myasthenia gravis as depression has been highlighted.[3] 20% of people with myasthenia gravis are initially diagnosed as having a psychiatric disorder,[4] and improvements in depressive symptoms associated with improvements in myasthenia gravis have been reported.[1,5] Whether depressive symptoms in individual cases are attributable to myasthenia gravis or major depressive disorder should be investigated. Since the AchR-Ab titre and the depressive symptoms improved over time in our case, we concluded that the patient's depressive symptoms could predominantly be attributed to myasthenia gravis. When managing treatment-resistant depressive patients, the medical history must be sufficiently considered.

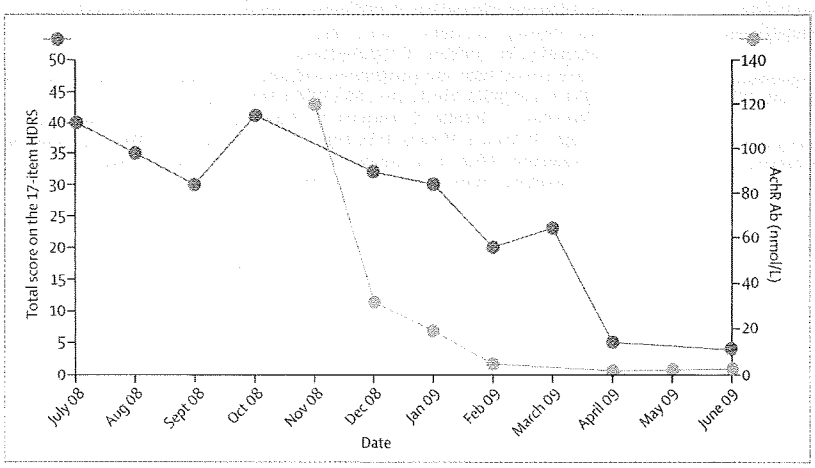

Figure: Changes in AchR-Ab titres and total-HDRS

Contributors

All the authors participated in the management of the patient. NO wrote the Case Report. Written consent to publish was obtained.

Acknowledgments

We thank T Nakai and M Sekine for temporary patient management.

References

1 Köhler W. Psychosocial aspects in patients with myasthenia gravis. *J Neurol* 2007; 254 (suppl 2): II90–92.

2 Pande AC, Grunhaus LJ. ECT for depression in the presence of myasthenia gravis. *Convuls Ther* 1990; 6: 172–75.

3 Kulaksizoglu IB. Mood and anxiety disorders in patients with myasthenia gravis: aetiology, diagnosis and treatment. *CNS Drugs* 2007; 21: 473–81.

4 Rohr W. Myasthenia gravis in the frontier of psychiatric diagnosis. *Psychiatr Prax* 1992; 19: 157–63.

5 Shinkai K, Ohmori O, Ueda N, et al. A case of myasthenia gravis preceded by major depression. *J Neuropsychiatry Clin Neurosci* 2001; 13: 116–17.

Progress in Neuro-Psychopharmacology & Biological Psychiatry xxx (2010) xxx–xxx

Contents lists available at ScienceDirect

Progress in Neuro-Psychopharmacology & Biological Psychiatry

journal homepage: www.elsevier.com/locate/pnp

Association analysis of *GRM2* and *HTR2A* with methamphetamine-induced psychosis and schizophrenia in the Japanese population

Tomoko Tsunoka [a,1], Taro Kishi [a,*], Tsuyoshi Kitajima [a,1], Tomo Okochi [a], Takenori Okumura [a], Yoshio Yamanouchi [a], Yoko Kinoshita [a], Kunihiro Kawashima [a], Hiroshi Naitoh [a], Toshiya Inada [b,c], Hiroshi Ujike [b,d], Mitsuhiko Yamada [b,e], Naohisa Uchimura [b,f], Ichiro Sora [b,g], Masaomi Iyo [b,h], Norio Ozaki [b,i], Nakao Iwata [a,b]

[a] *Department of Psychiatry, Fujita Health University School of Medicine, Toyoake, Aichi 470-1192, Japan*
[b] *Japanese Genetics Initiative for Drug Abuse, Japan*
[c] *Department of Psychiatry, Seiwa Hospital, Institute of Neuropsychiatry, Tokyo 162-0851, Japan*
[d] *Department of Neuropsychiatry, Okayama University Graduate School of Medicine, Dentistry and Pharmaceutical Sciences, 2-5-1 Shikata-cho, Okayama 700-8558, Japan*
[e] *National Institute of Mental Health, National Center of Neurology and Psychiatry, Ichikawa 272-0827, Japan*
[f] *Department of Neuropsychiatry, Kurume University School of Medicine, Kurume 830-0011, Japan*
[g] *Department of Psychobiology, Department of Neuroscience, Tohoku University Graduate School of Medicine, Sendai 980-8576, Japan*
[h] *Department of Psychiatry, Chiba University Graduate School of Medicine, Chiba 260-8677, Japan*
[i] *Department of Psychiatry, Nagoya University Graduate School of Medicine, Nagoya 466-8850, Japan*

ARTICLE INFO

Article history:
Received 9 December 2009
Received in revised form 24 February 2010
Accepted 2 March 2010
Available online xxxx

Keywords:
Methamphetamine-induced psychosis
Schizophrenia
Glutamate metabotropic receptor 2 gene (*GRM2*)
Serotonin receptor 2A gene (*HTR2A*)
Linkage disequilibrium
Tagging SNP
Functional SNP

ABSTRACT

Background: Abnormalities in glutaminergic neural transmission have been suggested to be involved in the pathogenesis of schizophrenia. A recent study reported that alterations in the 5-HT2A–mGluR2 complex may be involved in neural transmission in the schizophrenic cortex. In addition, methamphetamine-induced psychosis is thought to be similar to schizophrenia. Therefore, we conducted a case-control study with Japanese samples (738 schizophrenia patients, 196 methamphetamine-induced psychosis patients, and 802 controls) to evaluate the association and interaction between *GRM2*, *HTR2A* and schizophrenia.
Methods: We selected three 'tagging SNPs' in *GRM2*, and two biologically functional SNPs in *HTR2A* (T102C and A1438G), for the association analysis.
Results: We detected a significant association between methamphetamine-induced psychosis and *GRM2* in a haplotype-wise analysis, but not *HTR2A*. We did not detect an association between *GRM2* or *HTR2A* and schizophrenia. In addition, no interactions of *GRM2* and *HTR2A* were found in methamphetamine-induced psychosis or schizophrenia. We did not detect any novel polymorphisms in *GRM2* when we performed a mutation search using methamphetamine-induced psychosis samples.
Conclusion: Our results suggested that *GRM2* may play a role in the pathophysiology of methamphetamine-induced psychosis but not schizophrenia in the Japanese population. A replication study using larger samples or samples of other populations will be required for conclusive results.

1. Introduction

The glutamate hypothesis for the pathophysiology of schizophrenia is well-known (Weinberger, 2007). A recent clinical study also showed that LY379268, an agonist of the metabotropic glutamate 2/3 receptor (mGluR2/3), which belongs to group II mGluR, regulates glutamate neurotransmission through a presynaptic negative regulatory mechanism (Patil et al., 2007). LY379268 also has been shown to have an effect on psychotic symptoms in schizophrenia that is almost equivalent to the effect with olanzapine (Patil et al., 2007).

Recently, the hyperactivity of mGluR3 knockout mice (induced by amphetamine) was shown to be a reverse abnormal behavior mediated by LY379268 (Woolley et al., 2008). However, LY379268 did not correct the abnormal behavior of these mGluR2 knockout mice (Woolley et al., 2008). This result might show that mGluR2 is a more important therapeutic target than mGluR3 for the antipsychotic effect of LY379268 (Woolley et al., 2008).

Another recent animal study showed that mGluR2 and serotonin 2A receptor (5-HT2A) form complexes that mediate alterations in cellular response in the brain, and that these alterations were reversed by

Abbreviations: mGluR2/3, metabotropic glutamate 2/3 receptor; 5-HT2A, serotonin 2A receptor; LSD, lysergic acid diethylamide; *HTR2A*, 5-HT2A gene; *GRM2*, mGluR2 gene; METH, methamphetamine; SD, standard deviation; JGIDA, Japanese Genetics Initiative for Drug Abuse; LD, linkage disequilibrium; MAFs, minor allele frequencies; dHPLC, denaturing high performance liquid chromatography; HWE, Hardy–Weinberg equilibrium; MDR, multifactor dimensionality reduction; CD–CV hypothesis, common disease–common variants hypothesis; *GRM3*, mGluR3 gene.

* Corresponding author. Tel.: +81 562 93 9250; fax: +81 562 93 1831.
E-mail address: tarok@fujita-hu.ac.jp (T. Kishi).
[1] These authors contributed equally to this work.

0278-5846/$ – see front matter © 2010 Published by Elsevier Inc.
doi:10.1016/j.pnpbp.2010.03.002

mGluR2 antagonist (Gonzalez-Maeso et al., 2008). This was supported by evidence from a postmortem study using schizophrenia patients untreated by antipsychotics, who showed increased 5-HT2A and decreased mGluR2 in the cortex compared with age and gender match control samples (Gonzalez-Maeso et al., 2008). These findings suggest that abnormality of mGluR2 and 5-HT2A complexes might be involved in the pathophysiology for schizophrenia (Gonzalez-Maeso et al., 2008; Snyder, 2008).

Several genetic studies have reported an association between the 5-HT2A gene (*HTR2A*) and schizophrenia (Abdolmaleky et al., 2004; Baritaki et al., 2004; Golimbet et al., 2007; Inayama et al., 1996). However, other studies showed no association (Basile et al., 2001; Dominguez et al., 2007; Ertugrul et al., 2004; Pae et al., 2005; Sanders et al., 2008; Zhang et al., 2004). Moreover, only one genetic study detected no association between the mGluR2 gene (*GRM2*) and Japanese schizophrenia (Joo et al., 2001). Several genome-wide association studies (GWASs) reported that *HTR2A* and *GRM2* were not associated with schizophrenia (Holmans et al., 2009; Kirov et al., 2009; Moskvina et al., 2009; O'Donovan et al., 2008; O'Donovan et al., 2009; Purcell et al., 2009; Stefansson et al., 2009) or substance dependence (Chen et al., 2009). However, since schizophrenia is a complex disease, it seemed to us that evaluation of gene–gene interactions of *HTR2A* and *GRM2* in relation to the pathophysiology of schizophrenia was necessary.

LY379268 significantly inhibited hyperlocomotion in mice induced by methamphetamine (METH) (Satow et al., 2008). This animal model is considered to reflect the positive symptoms of schizophrenia. The symptoms of METH-induced psychosis are similar to those of paranoid type schizophrenia (Sato et al., 1992), which may indicate that METH-induced psychosis and schizophrenia have common susceptibility genes (Bousman et al., 2009). In support of this hypothesis, we reported that the V-act murine thymoma viral oncogene homologue 1 (AKT1) gene was associated with METH-induced psychosis (Ikeda et al., 2006) and schizophrenia (Ikeda et al., 2004) in the Japanese population. Furthermore, we performed an association analysis of these genes with methamphetamine (METH)-induced psychosis, since METH-induced psychosis is similar to schizophrenia (Sato et al., 1983).

GRM2 (OMIM *604099, 5 exons in this genomic region spanning 10.466 kb) and *HTR2A* (OMOM *182135, 3 exons in this genomic region spanning 63.463 kb) are located on 3p and 13q, respectively. The locations of these genomic regions were shown to be in a susceptibility region for schizophrenia (Badner and Gershon, 2002; Hovatta et al., 1998; Lewis et al., 2003; Maziade et al., 2001; Pulver et al., 1995). Therefore, we conducted a case-control study using Japanese schizophrenia and METH-induced psychosis samples.

2. Materials and methods

2.1. Subjects

The subjects were 738 schizophrenia patients (395 males and 343 females; mean age ± standard deviation (SD) 41.2 ± 13.8 years), 196 METH-induced psychosis and METH-dependence patients (163 males and 33 females; mean age ± SD 37.0 ± 10.8 years) and 802 healthy controls (351 males and 451 females; 37.6 ± 14.3 years). All the patients examined in this study suffered not only from METH-induced psychosis but also METH dependence. Consensus diagnoses of methamphetamine psychosis were made by two trained psychiatrists according to the ICD-10-DCR criteria (F15.2 and F15.5) on the basis of interviews and medical records. The patients with methamphetamine psychosis in the present study usually showed predominant positive symptoms such as delusion and hallucination. We excluded cases in which the predominant symptoms were of the negative and/or disorganized type in order to maintain the homogeneity of the patient group. The patients were categorized by prognosis into two types, a transient type and a prolonged type, based on the duration of the psychotic state after METH discontinuance. The transient type of patient was defined as a patient whose symptoms improved within 1 month after METH discontinuance and the start of treatment with antipsychotic, and the prolonged type was defined as a patient whose psychosis continued for more than 1 month after METH discontinuance and the start of treatment with an antipsychotic. In this study, there were 112 patients (56.9%) with the transient type and 85 patients (43.1%) with the prolonged type patients of METH psychosis. Cannabinoids were the most frequency abused drugs (31.4%), followed by cocaine (9.09%), LSD (9.09%), opioids (7.69%), and hypnotics (7.69%). Subjects with METH-use disorder were excluded if they had a clinical diagnosis of psychotic disorder, mood disorder, anxiety disorder, or eating disorder. More detailed characterizations of these subjects have been published elsewhere (Kishi et al., 2008, 2009b).

All healthy controls were also psychiatrically screened based on unstructured interviews including current and past psychiatric history. None had severe medical complications such as cirrhosis, renal failure, heart failure or other Axis-I disorders according to DSM-IV. No structured methods were used to assess psychiatric symptoms in the controls, which included hospital staff and medical students. Written informed consent was obtained from each subject. This study was approved by the ethics committees at Fujita Health University and Nagoya University Graduate School of Medicine, and by each participating member of the Institute of the Japanese Genetics Initiative for Drug Abuse (JGIDA).

2.2. SNP selection and linkage disequilibrium (LD) evaluation

We first consulted the HapMap database (release#23.a.phase2, Mar 2008, www.hapmap.org, population: Japanese Tokyo: minor allele frequencies (MAFs) of more than 0.05) and included 4 SNPs covering *GRM2* (5′-flanking regions including about 6.3 kb from the initial exon and about 1 kb downstream (3′) from the last exon: HapMap database contig number chr17: 51711684.. 51730152). Then three 'tagging SNPs' were selected with the criteria of an r^2 threshold greater than 0.8 in 'pair-wise tagging only' mode using the 'Tagger' program (Paul de Bakker, http://www/broad.mit.edu/mpg/tagger), an implement of the HAPLOVIEW software program (Barrett et al., 2005), for the following association analysis. *HTR2A* has been reported to have two biologically functional SNPs (T102C: rs6313, A1438G: rs6311) (Myers et al., 2007; Spurlock et al., 1998). According to the HapMap database, LD in these two SNPs in *HTR2A* was $r^2 = 0.770$; therefore, we performed an association analysis for these SNPs in this study.

2.3. SNP genotyping

We used TaqMan assays (ABI: Applied Biosystems, Inc., Foster City, CA,) for all SNPs. One allelic probe was labeled with FAM dye and the other with fluorescent VIC dye. The plates were heated for 2 min at 50 °C and 95 °C for 10 min, followed by 45 cycles of 95 °C for 15 s and 58 °C for 1 min. Please refer to ABI for the primer sequence. Detailed information, including primer sequences and reaction conditions, can be seen in our previous papers (Kishi et al., 2009b,d; Tsunoka et al., 2009).

2.4. Mutation screening

We detected significant association between *GRM2* and METH-induced psychosis. Therefore, we performed mutation screening with *GRM2* divided into 17 parts (promoter region, all exons including branch site) using 32 METH-induced psychosis patients (16 males and 16 females) and the primer extension method. Denaturing high performance liquid chromatography (dHPLC) analysis was carried out

Please cite this article as: Tsunoka T, et al, Association analysis of *GRM2* and *HTR2A* with methamphetamine-induced psychosis and schizophrenia in the Japanese population, Prog Neuro-Psychopharmacol Biol Psychiatry (2010), doi:10.1016/j.pnpbp.2010.03.002

to detect mutation. DNA sequencing was then performed using a 3100-Avant Genetic Analyzer (Applied Biosystems, CA). Primers were designed to cover the coding regions, the splice sites and approximately 1.0 kb of the 5′UTR and 500 bp of the 3′UTR of *GRM2*, using the Primer 3 primer design program (http://www.broad.mit.edu/ cgi-bin/primer/primer3_www.cgi) (Rozen and Skaletsky, 2000). A more detailed description of the methods can be seen in a previous paper (Suzuki et al., 2003). Detailed information, including primer sequence, is available on request.

2.5. Statistical analysis

Genotype deviation from the Hardy–Weinberg equilibrium (HWE) was evaluated by chi-square test (SAS/Genetics, release 8.2, SAS Japan Inc., Tokyo, Japan). Marker-trait association analysis was used to evaluate allele- and genotype-wise association with the chi-square test (SAS/Genetics, release 8.2, SAS Japan Inc., Tokyo, Japan). The distribution of patient characteristics in the schizophrenia group, METH-induced psychosis group and healthy control group was analyzed using a *t* test or a chi-square test. We found significant differences in gender distribution among these groups ($P_{\text{schizophrenia}} \leq 0.001$ and $P_{\text{METH-induced psychosis}} \leq 0.001$), however, there was no difference in age among them ($P_{\text{schizophrenia}} = 0.238$ and $P_{\text{METH-induced psychosis}} = 0.765$). We therefore performed logistic regression analysis to compare the phenotype of each of the examined SNPs genotypes to adjust for possible confounding. The phenotype (each disorder or control) was the dependent variable, and gender, age at the time of recruitment and each examined SNP genotype were set as the independent variables. The statistical package JMP for windows was used for logistic regression analysis (JMP 5.0. 1J, SAS Japan Inc., Tokyo, Japan). Haplotype-wise association analysis was evaluated with a likelihood ratio test using the COCAPHASE2.403 program (Dudbridge, 2003). This software uses the EM algorithm to estimate the haplotype frequencies of unphased genotype data and standard unconditional logistic regression analysis, applying the likelihood ratio test under a log-linear model to compare haplotype frequencies between cases and controls. In order to avoid misleading results caused by rare haplotypes, all haplotypes with a frequency less than or equal to 5% in both the cases and the controls were declared rare and clumped together for a test of the null hypothesis, using the command line option 'rare 0.05.' This analysis adjusted for age and gender. To control inflation of the type I error rate, we used Bonferroni's correction. Power calculation was performed using a genetic power calculator (Purcell et al., 2003). We set each item in each value in the Genetic Power Calculator as follows: prevalence: 0.01 in schizophrenia and METH-induced psychosis, User-defined: 0.01 (5 SNPs examined in this study. Bonferroni's correction was used to control inflation of the type I error rate).

The significance level for all statistical tests was 0.05.

3. Results

The LD structure in *GRM2* from the HapMap database can be seen in our previous paper (Tsunoka et al., 2009). Genotype frequencies of all SNPs were in HWE (Table 1). In addition, we added twenty-five randomly selected samples that were genotyped again as a measure of genotyping quality control, and the genotype consistency rates for all four SNPs were 100% (Tsunoka et al., 2009). We detected a significant association between *GRM2* and METH-induced psychosis in the allele/genotype-wise analysis with the chi-square test but not with logistic regression adjusted for age and gender (Tables 1 and 2). In addition, we found an association between *GRM2* and METH-induced psychosis in the haplotype-wise analysis adjusting age and gender (Tables 3). However, *HTR2A* was not associated with schizophrenia or METH-induced psychosis (Tables 1–3). Although we performed mutation screening for *GRM2* using METH-induced psychosis samples, we did not detect any novel polymorphisms in *GRM2* in the METH-induced psychosis samples.

To evaluate the interactions with each SNP in these genes, we analyzed the gene–gene interactions with the use of the Multifactor Dimensionality Reduction (MDR) method (Hahn et al., 2003). In this study, each of the genotype variables in one dimension were assessed to determine test accuracy (defined as mean sensitivity and specificity) in terms of predicting delivery type using 10-fold cross-validation for each disorder and control. MDR analysis was performed using MDR software (v 1.0.0; http://www.epistasis.org/). In this analysis, however, no interactions were found in METH-induced psychosis and schizophrenia (data not shown).

In the power analysis, we obtained more than 80% power for the detection of association when we set the genotype relative risk at 1.45–1.90 and 1.32–1.60 in METH-induced psychosis and schizophrenia, respectively, for *GRM2*, and at 1.45–1.47 and 1.27–1.32 in METH-induced psychosis and schizophrenia, respectively, for *HTR2A* under a multiplicative model of inheritance.

Table 1
Association analysis of single markers in *HTR2A* and *GRM2* with schizophrenia and methamphetamine-induced psychosis.

Gene	SNP ID	Phenotype[a]	MAFs[b]	N	Genotype distribution[c]				*P*-value[e]		Corrected *P*-value[e,f]	
					M/M	M/m	m/m	HWE[d]	Genotype	Allele	Genotype	Allele
HTR2A	rs6311	Controls	0.440	802	262	374	166	0.128				
	−1438A/G	Schizophrenia	0.409	738	264	344	130	0.328	0.225	0.0828		
		METH-induced psychosis	0.459	196	58	96	42	0.846	0.708	0.497		
	rs6313	Controls	0.485	802	220	386	196	0.301				
	102T/C	Schizophrenia	0.5	738	182	374	182	0.713	0.440	0.407		
		METH-induced psychosis	0.492	196	52	95	49	0.671	0.965	0.795		
GRM2	rs3821829	Controls	0.0468	802	731	67	4	0.0751				
	C>T	Schizophrenia	0.0420	738	676	62	0	0.234	0.158	0.523		
		METH-induced psychosis	0.0408	196	181	14	1	0.219	0.856	0.613		
	rs12487957	Controls	0.333	802	346	378	78	0.0834				
	T>C	Schizophrenia	0.308	738	354	314	70	0.976	0.150	0.132		
		METH-induced psychosis	0.258	196	106	79	11	0.453	**0.0126**	**0.00413**	0.0630	**0.0207**
	rs4687771	Controls	0.376	802	300	401	101	0.0632				
	T>A	Schizophrenia	0.360	738	299	347	92	0.574	0.435	0.352		
		METH-induced psychosis	0.281	196	100	82	14	0.612	**0.00116**	**0.000414**	**0.00580**	**0.00207**

[a] SCZ: schizophrenia METH psychosis: methamphetamine-induced psychosis.
[b] MAFs: minor allele frequencies.
[c] M: major allele, m: minor allele.
[d] Hardy–Weinberg equilibrium.
[e] Bold numbers represent significant *P*-value.
[f] Calculated by Bonferroni's correction.

Please cite this article as: Tsunoka T, et al, Association analysis of *GRM2* and *HTR2A* with methamphetamine-induced psychosis and schizophrenia in the Japanese population, Prog Neuro-Psychopharmacol Biol Psychiatry (2010), doi:10.1016/j.pnpbp.2010.03.002

Table 2
Logistic regression analysis of single markers in *HTR2A* and *GRM2* with schizophrenia and methamphetamine-induced psychosis.

Gene	SNP ID	Genotype	Schizophrenia			METH-induced psychosis[a]		
			P-value	OR[b]	95% CI[c]	*P*-value	OR[b]	95% CI[c]
HTR2A	rs6311	AG	0.853	1.03	0.340–2.22	0.924	0.836	0.760–1.40
	−1438A/G	GG	0.978	1.23	0.618–1.55	0.579	0.291	0.839–1.81
	rs6313	TC	1.02	0.965	0.646–1.60	0.940	0.817	0.716–1.31
	102T/C	CC	1.07	0.961	0.633–1.83	0.801	0.826	0.676–1.37
	rs3821829	CT	1.42	0.889	0.160–7.45	0.702	0.703	0.539–1.22
	C>T	TT	0.486	0.909	0.0288–30.2	0.659	0.709	0.557–1.44
GRM2	rs12487957	TC	1.02	1.23	0.556–1.81	0.956	0.241	0.869–1.74
	T>C	CC	2.21	1.19	0.923–5.91	0.0912	0.506	0.717–1.98
	rs4687771	TA	1.14	1.04	0.649–1.95	0.648	0.797	0.754–1.45
	T>A	AA	2.01	1.27	0.910–4.82	0.0986	0.314	0.802–2.01

Reference genotypes are common genotype. Adjustment for age and gender.
[a] METH-induced psychosis: methamphetamine-induced psychosis.
[b] OR: odds ratio.
[c] CI: confidential interval.

4. Discussion

In the single marker association study, we detected a significant association between *GRM2* and METH-induced psychosis with chi-square test. However, this association may have been due to biased samples, which is unmatched for age. We therefore performed a logistic regression analysis to compare the phenotypes of each of the examined SNPs genotypes, using several clinical factors as other independent variables to adjust for possible confounding. Although we did not detect an association between the three tagging SNP genotypes in *GRM2* and METH-induced psychosis with logistic regression analysis, we found an association between *GRM2* and METH-induced psychosis in the haplotype-wise analysis adjusting for age and gender. Our results therefore suggest that *GRM2* plays a role in the pathophysiology of METH-induced psychosis in the Japanese population. We did not detect novel polymorphisms, although we performed a mutation search for *GRM2* (promoter region, all exons including branch site) using METH-induced psychosis samples.

We designed the study design based on the common disease–common variants hypothesis (CD–CV hypothesis) (Chakravarti, 1999). A recent study has shown associations between common diseases such as schizophrenia and rare variants (Weickert et al., 2008). If the genetic background of METH-induced psychosis is described by the common disease–rare variants hypothesis, further investigation, such as medical resequencing using larger samples, will be required. Moreover, mGluR2/3 agonist has been observed to have certain antipsychotic effects (Patil et al., 2007), and the mGluR3 gene (*GRM3*) has been considered a good candidate gene for the pathogenesis of METH-induced psychosis. Further investigations will be necessary to analyze gene–gene interactions between *GRM2* and *GRM3* in METH-induced psychosis.

It has also been suggested that alterations in mGluR2 and the 5-HT2A complex might be involved in the pathophysiology of schizophrenia. Because 5-HT2A receptors are one of the major pharmacological therapeutic targets of atypical antipsychotics, the pharmacogenomics of psychotic disorders (response to antipsychotics) will also need to be investigated in the future.

In this study, we found an association between *GRM2* and METH psychosis but not schizophrenia in the Japanese population. METH psychosis has long been considered a pharmacologic model of schizophrenia (Snyder, 1973; Ujike, 2002). To date, several genes have been reported to have an association with METH psychosis (Ikeda et al., 2006; Kishi et al., 2009a,c; Kishimoto et al., 2008a,b; Kotaka et al., 2009; Morita et al., 2008; Otani et al., 2008; Ujike et al., 2009). However, only a few of these genes have been found to be associated with Japanese schizophrenia (Ikeda et al., 2006; Kishimoto et al., 2008a). One of the reasons for the inconsistent results among these studies is considered to be the difference in sample size among the studies of these disorders. A replication study using larger samples or samples of other populations will be required for conclusive results (Bousman et al., 2009).

A few points of caution should be mentioned with respect to our results. First, the positive association may be due to biased samples,

Table 3
All markers haplotype-wise analysis of *HTR2A* and *GRM2*.

Gene	Marker	Phenotype[a]	Haplotype frequency	OR[b]	95% CI[c]	Individual haplotype *P*-value[b]	Phenotype[a]	Global *P*-value[b]	Corrected global *P*-value[b,c]
HTR2A	A–T	Control	0.0778						
rs6311–rs6313		Schizophrenia	0.100	1.37	0.908–2.06	0.177			
		METH-induced psychosis	0.0830	1.39	0.750–2.58	0.327			
	G–T	Control	0.467				Schizophrenia	0.298	
		Schizophrenia	0.430	1.00	1.00–1.00	0.212			
		METH-induced psychosis	0.465	1.01	0.698–1.71	0.468			
	G–C	Control	0.455				METH-induced psychosis	0.589	
		Schizophrenia	0.470	1.11	0.825–1.45	0.653			
		METH-induced psychosis	0.452	1.02	0.498–1.89	0.922			
GRM2	C–C–A	Control	0.673						
rs3821829–rs12487957–rs4687771		Schizophrenia	0.659	1.00	1.00–1.00	0.424	Schizophrenia	0.424	
		METH-induced psychosis	0.746	1.00	1.00–1.00	**0.00822**			
	C–T–T	Control	0.327						
		Schizophrenia	0.341	1.07	0.909–1.26	0.424	METH-induced psychosis	**0.00746**	**0.0149**
		METH-induced psychosis	0.254	0.686	0.518–0.908	**0.00822**			

[a] SCZ: schizophrenia METH psychosis: methamphetamine-induced psychosis.
[b] Bold numbers represent significant *P*-value.
[c] Calculated by Bonferroni correction.

Please cite this article as: Tsunoka T, et al, Association analysis of *GRM2* and *HTR2A* with methamphetamine-induced psychosis and schizophrenia in the Japanese population, Prog Neuro-Psychopharmacol Biol Psychiatry (2010), doi:10.1016/j.pnpbp.2010.03.002

such as unmatched gender samples, or small sample size. On average, the METH-induced psychosis patients were much younger than the controls. We therefore performed a logistic regression analysis to compare the phenotypes of each of the examined SNPs genotypes, using several clinical factors as other independent variables to adjust for possible confounding. Our control samples for 3SNPs in *GRM2* were within a limit that satisfies HWE. The positive association with METH-induced psychosis could be due to type I error, possibly because of population stratification. However, another recent study confirmed that there is no population stratification in our control samples (Ikeda et al., 2009). In addition, we added twenty-five randomly selected samples that were genotyped again as a measure of genotyping quality control, and the genotype consistency rates for all four SNPs were 100% (Tsunoka et al., 2009). Second, we did not include a mutation scan to detect rare variants with functional effects for schizophrenia. However, Joo et al. reported no association of *GRM2* with Japanese schizophrenia after mutation screening for *GRM2* (Joo et al., 2001). In addition, it is difficult to evaluate the association of rare variants, unless statistical power is obtained. To overcome these limitations, a replication study using larger samples or samples of other populations will be required for conclusive results (Bousman et al., 2009).

5. Conclusion

In conclusion, our results suggest that *GRM2* may play a major role in the pathophysiology of METH-induced psychosis but not schizophrenia in the Japanese population. However, an interaction between mGluR2 and 5-HT2A seen in an animal study was not detected with these genes levels.

Acknowledgements

We thank Ms. M. Miyata, and Ms. S. Ishihara for their technical support. This work was supported in part by research grants from the Japan Ministry of Education, Culture, Sports, Science and Technology, the Ministry of Health, Labor and Welfare, and the Health Sciences Foundation (Research on Health Sciences focusing on Drug Innovation).

References

Abdolmaleky HM, Faraone SV, Glatt SJ, Tsuang MT. Meta-analysis of association between the T102C polymorphism of the 5HT2a receptor gene and schizophrenia. Schizophr Res 2004;67:53–62.
Badner JA, Gershon ES. Meta-analysis of whole-genome linkage scans of bipolar disorder and schizophrenia. Mol Psychiatry 2002;7:405–11.
Baritaki S, Rizos E, Zafiropoulos A, Soufla G, Katsafouros K, Gourvas V, et al. Association between schizophrenia and DRD3 or HTR2 receptor gene variants. Eur J Hum Genet 2004;12:535–41.
Barrett JC, Fry B, Maller J, Daly MJ. Haploview: analysis and visualization of LD and haplotype maps. Bioinformatics 2005;21:263–5.
Basile VS, Masellis M, McIntyre RS, Meltzer HY, Lieberman JA, Kennedy JL. Genetic dissection of atypical antipsychotic-induced weight gain: novel preliminary data on the pharmacogenetic puzzle. J Clin Psychiatry 2001;62(Suppl 23):45–66.
Bousman CA, Glatt SJ, Everall IP, Tsuang MT. Genetic association studies of methamphetamine use disorders: a systematic review and synthesis. Am J Med Genet B Neuropsychiatr Genet 2009.
Chakravarti A. Population genetics—making sense out of sequence. Nat Genet 1999;21:56–60.
Chen X, Cho K, Singer BH, Zhang H. PKNOX2 gene is significantly associated with substance dependence in European-origin women. Proc Natl Acad Sci U S A 2009.
Dominguez E, Loza MI, Padin F, Gesteira A, Paz E, Paramo M, et al. Extensive linkage disequilibrium mapping at HTR2A and DRD3 for schizophrenia susceptibility genes in the Galician population. Schizophr Res 2007;90:123–9.
Dudbridge F. Pedigree disequilibrium tests for multilocus haplotypes. Genet Epidemiol 2003;25:115–21.
Ertugrul A, Kennedy JL, Masellis M, Basile VS, Jayathilake K, Meltzer HY. No association of the T102C polymorphism of the serotonin 2A receptor gene (HTR2A) with suicidality in schizophrenia. Schizophr Res 2004;69:301–5.
Golimbet VE, Lavrushina OM, Kaleda VG, Abramova LI, Lezheiko TV. Supportive evidence for the association between the T102C 5-HTR2A gene polymorphism and schizophrenia: a large-scale case-control and family-based study. Eur Psychiatry 2007;22:167–70.
Gonzalez-Maeso J, Ang RL, Yuen T, Chan P, Weisstaub NV, Lopez-Gimenez JF, et al. Identification of a serotonin/glutamate receptor complex implicated in psychosis. Nature 2008;452:93–7.
Hahn LW, Ritchie MD, Moore JH. Multifactor dimensionality reduction software for detecting gene–gene and gene–environment interactions. Bioinformatics 2003;19:376–82.
Holmans PA, Riley B, Pulver AE, Owen MJ, Wildenauer DB, Gejman PV, et al. Genomewide linkage scan of schizophrenia in a large multicenter pedigree sample using single nucleotide polymorphisms. Mol Psychiatry 2009;14:786–95.
Hovatta I, Lichtermann D, Juvonen H, Suvisaari J, Terwilliger JD, Arajarvi R, et al. Linkage analysis of putative schizophrenia gene candidate regions on chromosomes 3p, 5q, 6p, 8p, 20p and 22q in a population-based sampled Finnish family set. Mol Psychiatry 1998;3:452–7.
Ikeda M, Iwata N, Suzuki T, Kitajima T, Yamanouchi Y, Kinoshita Y, et al. Association of AKT1 with schizophrenia confirmed in a Japanese population. Biol Psychiatry 2004;56:698–700.
Ikeda M, Iwata N, Suzuki T, Kitajima T, Yamanouchi Y, Kinoshiya Y, et al. Positive association of AKT1 haplotype to Japanese methamphetamine use disorder. Int J Neuropsychopharmacol 2006;9:77–81.
Ikeda M, Aleksic B, Kirov G, Kinoshita Y, Yamanouchi Y, Kitajima T, et al. Copy number variation in schizophrenia in the Japanese population. Biol Psychiatry 2009.
Inayama Y, Yoneda H, Sakai T, Ishida T, Nonomura Y, Kono Y, et al. Positive association between a DNA sequence variant in the serotonin 2A receptor gene and schizophrenia. Am J Med Genet 1996;67:103–5.
Joo A, Shibata H, Ninomiya H, Kawasaki H, Tashiro N, Fukumaki Y. Structure and polymorphisms of the human metabotropic glutamate receptor type 2 gene (GRM2): analysis of association with schizophrenia. Mol Psychiatry 2001;6:186–92.
Kirov G, Zaharieva I, Georgieva L, Moskvina V, Nikolov I, Cichon S, et al. A genome-wide association study in 574 schizophrenia trios using DNA pooling. Mol Psychiatry 2009;14:796–803.
Kishi T, Ikeda M, Kitajima T, Yamanouchi Y, Kinoshita Y, Kawashima K, et al. Alpha4 and beta2 subunits of neuronal nicotinic acetylcholine receptor genes are not associated with methamphetamine-use disorder in the Japanese population. Ann N Y Acad Sci 2008;1139:70–82.
Kishi T, Ikeda M, Kitajima T, Yamanouchi Y, Kinoshita Y, Kawashima K, et al. A functional polymorphism in estrogen receptor alpha gene is associated with Japanese methamphetamine induced psychosis. Prog Neuropsychopharmacol Biol Psychiatry 2009a;33:895–8.
Kishi T, Kitajima T, Tsunoka T, Ikeda M, Yamanouchi Y, Kinoshita Y, et al. Genetic association analysis of serotonin 2A receptor gene (HTR2A) with bipolar disorder and major depressive disorder in the Japanese population. Neurosci Res 2009b;64:231–4.
Kishi T, Tsunoka T, Ikeda M, Kitajima T, Kawashima K, Okochi T, et al. Serotonin 1A receptor gene is associated with Japanese methamphetamine-induced psychosis patients. Neuropharmacology 2009c.
Kishi T, Yoshimura R, Kitajima T, Okochi T, Okumura T, Tsunoka T, et al. HTR2A is associated with SSRI response in major depressive disorder in a Japanese cohort. Neuromolecular Med 2009d.
Kishimoto M, Ujike H, Motohashi Y, Tanaka Y, Okahisa Y, Kotaka T, et al. The dysbindin gene (DTNBP1) is associated with methamphetamine psychosis. Biol Psychiatry 2008a;63:191–6.
Kishimoto M, Ujike H, Okahisa Y, Kotaka T, Takaki M, Kodama M, et al. The Frizzled 3 gene is associated with methamphetamine psychosis in the Japanese population. Behav Brain Funct 2008b;4:37.
Kotaka T, Ujike H, Okahisa Y, Takaki M, Nakata K, Kodama M, et al. G72 gene is associated with susceptibility to methamphetamine psychosis. Prog Neuropsychopharmacol Biol Psychiatry 2009;33:1046–9.
Lewis CM, Levinson DF, Wise LH, DeLisi LE, Straub RE, Hovatta I, et al. Genome scan meta-analysis of schizophrenia and bipolar disorder, part II: schizophrenia. Am J Hum Genet 2003;73:34–48.
Maziade M, Roy MA, Rouillard E, Bissonnette L, Fournier JP, Roy A, et al. A search for specific and common susceptibility loci for schizophrenia and bipolar disorder: a linkage study in 13 target chromosomes. Mol Psychiatry 2001;6:684–93.
Morita Y, Ujike H, Tanaka Y, Kishimoto M, Okahisa Y, Kotaka T, et al. The glycine transporter 1 gene (GLYT1) is associated with methamphetamine-use disorder. Am J Med Genet B Neuropsychiatr Genet 2008;147B:54–8.
Moskvina V, Craddock N, Holmans P, Nikolov I, Pahwa JS, Green E, et al. Gene-wide analyses of genome-wide association data sets: evidence for multiple common risk alleles for schizophrenia and bipolar disorder and for overlap in genetic risk. Mol Psychiatry 2009;14:252–60.
Myers RL, Airey DC, Manier DH, Shelton RC, Sanders-Bush E. Polymorphisms in the regulatory region of the human serotonin 5-HT2A receptor gene (HTR2A) influence gene expression. Biol Psychiatry 2007;61:167–73.
O'Donovan MC, Craddock N, Norton N, Williams H, Peirce T, Moskvina V, et al. Identification of loci associated with schizophrenia by genome-wide association and follow-up. Nat Genet 2008;40:1053–5.
O'Donovan MC, Norton N, Williams H, Peirce T, Moskvina V, Nikolov I, et al. Analysis of 10 independent samples provides evidence for association between schizophrenia and a SNP flanking fibroblast growth factor receptor 2. Mol Psychiatry 2009;14:30–6.
Otani K, Ujike H, Sakai A, Okahisa Y, Kotaka T, Inada T, et al. Reduced CYP2D6 activity is a negative risk factor for methamphetamine dependence. Neurosci Lett 2008;434:88–92.
Pae CU, Artioli P, Serretti A, Kim TS, Kim JJ, Lee CU, et al. No evidence for interaction between 5-HT2A receptor and serotonin transporter genes in schizophrenia. Neurosci Res 2005;52:195–9.
Patil ST, Zhang L, Martenyi F, Lowe SL, Jackson KA, Andreev BV, et al. Activation of mGlu2/3 receptors as a new approach to treat schizophrenia: a randomized Phase 2 clinical trial. Nat Med 2007;13:1102–7.
Pulver AE, Lasseter VK, Kasch L, Wolyniec P, Nestadt G, Blouin JL, et al. Schizophrenia: a genome scan targets chromosomes 3p and 8p as potential sites of susceptibility genes. Am J Med Genet 1995;60:252–60.

Please cite this article as: Tsunoka T, et al, Association analysis of *GRM2* and *HTR2A* with methamphetamine-induced psychosis and schizophrenia in the Japanese population, Prog Neuro-Psychopharmacol Biol Psychiatry (2010), doi:10.1016/j.pnpbp.2010.03.002

Purcell S, Cherny SS, Sham PC. Genetic power calculator: design of linkage and association genetic mapping studies of complex traits. Bioinformatics 2003;19:149–50.
Purcell SM, Wray NR, Stone JL, Visscher PM, O'Donovan MC, Sullivan PF, et al. Common polygenic variation contributes to risk of schizophrenia and bipolar disorder. Nature 2009;460:748–52.
Rozen S, Skaletsky H. Primer3 on the WWW for general users and for biologist programmers. Methods Mol Biol 2000;132:365–86.
Sanders AR, Duan J, Levinson DF, Shi J, He D, Hou C, et al. No significant association of 14 candidate genes with schizophrenia in a large European ancestry sample: implications for psychiatric genetics. Am J Psychiatry 2008;165:497–506.
Sato M, Chen CC, Akiyama K, Otsuki S. Acute exacerbation of paranoid psychotic state after long-term abstinence in patients with previous methamphetamine psychosis. Biol Psychiatry 1983;18:429–40.
Sato M, Numachi Y, Hamamura T. Relapse of paranoid psychotic state in methamphetamine model of schizophrenia. Schizophr Bull 1992;18:115–22.
Satow A, Maehara S, Ise S, Hikichi H, Fukushima M, Suzuki G, et al. Pharmacological effects of the metabotropic glutamate receptor 1 antagonist compared with those of the metabotropic glutamate receptor 5 antagonist and metabotropic glutamate receptor 2/3 agonist in rodents: detailed investigations with a selective allosteric metabotropic glutamate receptor 1 antagonist, FTIDC [4-[1-(2-fluoropyridine-3-yl)-5-methyl-1H-1,2,3-triazol-4-yl]-N-isopropyl-N-methyl-3,6-dihydropyridine-1(2H)-carboxamide]. J Pharmacol Exp Ther 2008;326:577–86.
Snyder SH. Amphetamine psychosis: a "model" schizophrenia mediated by catecholamines. Am J Psychiatry 1973;130:61–7.
Snyder SH. Neuroscience: a complex in psychosis. Nature 2008;452:38–9.
Spurlock G, Heils A, Holmans P, Williams J, D'Souza UM, Cardno A, et al. A family based association study of T102C polymorphism in 5HT2A and schizophrenia plus identification of new polymorphisms in the promoter. Mol Psychiatry 1998;3:42–9.
Stefansson H, Ophoff RA, Steinberg S, Andreassen OA, Cichon S, Rujescu D, et al. Common variants conferring risk of schizophrenia. Nature 2009;460:744–7.
Suzuki T, Iwata N, Kitamura Y, Kitajima T, Yamanouchi Y, Ikeda M, et al. Association of a haplotype in the serotonin 5-HT4 receptor gene (HTR4) with Japanese schizophrenia. Am J Med Genet B Neuropsychiatr Genet 2003;121B:7–13.
Tsunoka T, Kishi T, Ikeda M, Kitajima T, Yamanouchi Y, Kinoshita Y, et al. Association analysis of Group II metabotropic glutamate receptor genes (GRM2 and GRM3) with mood disorders and fluvoxamine response in a Japanese population. Prog Neuropsychopharmacol Biol Psychiatry 2009;33:875–9.
Ujike H. Stimulant-induced psychosis and schizophrenia: the role of sensitization. Curr Psychiatry Rep 2002;4:177–84.
Ujike H, Katsu T, Okahisa Y, Takaki M, Kodama M, Inada T, et al. Genetic variants of D2 but not D3 or D4 dopamine receptor gene are associated with rapid onset and poor prognosis of methamphetamine psychosis. Prog Neuropsychopharmacol Biol Psychiatry 2009;33:625–9.
Weickert CS, Miranda-Angulo AL, Wong J, Perlman WR, Ward SE, Radhakrishna V, et al. Variants in the estrogen receptor alpha gene and its mRNA contribute to risk for schizophrenia. Hum Mol Genet 2008;17:2293–309.
Weinberger DR. Schizophrenia drug says goodbye to dopamine. Nat Med 2007;13:1018–9.
Woolley ML, Pemberton DJ, Bate S, Corti C, Jones DN. The mGlu2 but not the mGlu3 receptor mediates the actions of the mGluR2/3 agonist, LY379268, in mouse models predictive of antipsychotic activity. Psychopharmacology (Berl) 2008;196:431–40.
Zhang XN, Jiang SD, He XH, Zhang LN. 102T/C SNP in the 5-hydroxytryptamine receptor 2A (HTR2A) gene and schizophrenia in two southern Han Chinese populations: lack of association. Am J Med Genet B Neuropsychiatr Genet 2004;126B:16–8.

Please cite this article as: Tsunoka T, et al, Association analysis of *GRM2* and *HTR2A* with methamphetamine-induced psychosis and schizophrenia in the Japanese population, Prog Neuro-Psychopharmacol Biol Psychiatry (2010), doi:10.1016/j.pnpbp.2010.03.002

Schizophrenia Research xxx (2010) xxx–xxx

Contents lists available at ScienceDirect

Schizophrenia Research

journal homepage: www.elsevier.com/locate/schres

Failure to find an association between *myosin heavy chain 9, non-muscle* (*MYH9*) and schizophrenia: A three-stage case–control association study

Hideki Amagane [a,1], Yuichiro Watanabe [a,b,1], Naoshi Kaneko [a,*], Ayako Nunokawa [a], Tatsuyuki Muratake [c], Hiroki Ishiguro [d], Tadao Arinami [d], Hiroshi Ujike [e], Toshiya Inada [f], Nakao Iwata [g], Hiroshi Kunugi [h], Tsukasa Sasaki [i], Ryota Hashimoto [j], Masanari Itokawa [k], Norio Ozaki [l], Toshiyuki Someya [a]

[a] *Department of Psychiatry, Niigata University Graduate School of Medical and Dental Sciences, 757 Asahimachidori-ichibancho, Chuo-ku, Niigata 951-8510, Japan*
[b] *Health Administration Center, Niigata University, 8050 Ikarashi-ninocho, Nishi-ku, Niigata 950-2181, Japan*
[c] *Furumachi Mental Clinic, 608 Furumachidori-gobancho, Chuo-ku, Niigata 951-8063, Japan*
[d] *Department of Medical Genetics, Doctoral Program in Social and Environmental Medicine, Graduate School of Comprehensive Human Sciences, University of Tsukuba, 1-1-1 Tennodai, Tsukuba, Ibaraki 305-8575, Japan*
[e] *Department of Neuropsychiatry, Okayama University, Graduate School of Medicine, Dentistry and Pharmaceutical Sciences, 2-5-1 Shikata-cho, Okayama 700-8558, Japan*
[f] *Seiwa Hospital, Institute of Neuropsychiatry, 91 Bentencho, Shinjuku-ku, Tokyo 162-0851, Japan*
[g] *Department of Psychiatry, Fujita Health University School of Medicine, Toyoake, Aichi 470-1192, Japan*
[h] *Department of Mental Disorder Research, National Institute of Neuroscience, National Center of Neurology and Psychiatry, 4-1-1 Ogawahigashi, Kodaira, Tokyo 187-8502, Japan*
[i] *Health Service Center, University of Tokyo, 7-3-1 Hongo, Bunkyo-ku, Tokyo 113-8655, Japan*
[j] *The Osaka-Hamamatsu Joint Research Center for Child Mental Development, Osaka University Graduate School of Medicine, D3, 2-2, Yamadaoka, Suita, Osaka, 5650871, Japan*
[k] *Schizophrenia Research Project, Tokyo Institute of Psychiatry, 2-1-8 Kamikitazawa, Setagaya-ku, Tokyo 156-8585, Japan*
[l] *Department of Psychiatry, School of Medicine, Nagoya University, 65 Tsurumai-cho, Showa-ku, Nagoya, Aichi 466-8550, Japan*

ARTICLE INFO

Article history:
Received 30 October 2009
Received in revised form 26 January 2010
Accepted 27 January 2010
Available online xxxx

Keywords:
Chromosome 22
Case–control study
Japanese
MYH9
Schizophrenia

ABSTRACT

Several genome-wide linkage studies have suggested linkage between markers on the long arm of chromosome 22 and schizophrenia. It has also been reported that 22q11.2 deletions increase the risk of schizophrenia. Therefore, 22q is a candidate region for schizophrenia. To search for genetic susceptibility loci for schizophrenia on 22q, we conducted a three-stage case–control association study in Japanese individuals. In the first stage, we examined 13 microsatellite markers on 22q in 766 individuals (340 patients with schizophrenia and 426 control individuals) and found a potential association of AFM262VH5 (D22S283) with schizophrenia. In the second stage, we performed fine mapping of the *myosin heavy chain 9, non-muscle* (*MYH9*) gene, where AFM262VH5 is located, using 25 tagging single nucleotide polymorphisms (SNPs). We obtained potential associations between three SNPs in *MYH9* and schizophrenia in 1193 individuals (595 patients and 598 controls), which included the individuals analyzed in the first stage. In the third stage, however, we could not replicate these associations in 4694 independent individuals (2288 patients and 2406 controls). Our results suggest that *MYH9* does not confer increased susceptibility to schizophrenia in the Japanese population, although we could not exclude possible contributions of other genes on 22q to the pathogenesis of schizophrenia.

1. Introduction

Several genome-wide linkage studies have suggested linkage between markers on the long arm of chromosome 22 and schizophrenia (Blouin et al., 1998; DeLisi et al., 2002; Faraone et al., 2006; Williams et al., 2003). Two meta-analyses provided

* Corresponding author. Tel.: +81 25 227 2213; fax: +81 25 227-0777.
E-mail address: kane704@med.niigata-u.ac.jp (N. Kaneko).
[1] These authors contributed equally to this work.

0920-9964/$ – see front matter © 2010 Elsevier B.V. All rights reserved.
doi:10.1016/j.schres.2010.01.023

supportive evidence for susceptibility loci for schizophrenia on 22q (Badner and Gershon, 2002; Lewis et al., 2003), whereas a multicenter study and the most recent meta-analysis conducted both failed to find linkage of 22q to schizophrenia (Mowry et al., 2004; Ng et al., 2009). There is a higher incidence of schizophrenia among patients with velocardiofacial syndrome (Murphy et al., 1999; Shprintzen et al., 1992), which is associated with a hemizygous interstitial deletion of 22q11.2. It has been reported that interstitial deletion of 22q11.2 increases the risk of schizophrenia (Arinami, 2006; Karayiorgou et al., 1995), and this was confirmed by recent genome-wide surveys of rare copy number variants (International Schizophrenia Consortium, 2008; Xu et al., 2008). In addition, there are some interesting candidate genes for schizophrenia in this region including *proline dehydrogenase 1* (*PRODH*) (Liu et al., 2002), *catechol-O-methyltransferase* (*COMT*) (Shifman et al., 2002) and *zinc finger, DHHC-type containing 8* (*ZDHHC8*) (Mukai et al., 2004). Therefore, 22q is a candidate region for schizophrenia, although the results of previous studies are not necessarily consistent.

To search for genetic susceptibility loci for schizophrenia on 22q, we conducted a three-stage case–control association study in Japanese individuals. In the first stage, we examined 13 microsatellite markers on 22q in 766 individuals (340 patients with schizophrenia and 426 control individuals) and found a potential association of AFM262VH5 (D22S283) with schizophrenia. In the second stage, we performed a fine mapping of the *myosin heavy chain 9, non-muscle* (*MYH9*) gene, where AFM262VH5 is located, using 25 tagging single nucleotide polymorphisms (SNPs) in 1193 individuals (595 patients and 598 controls), which included the individuals analyzed in the first stage. In the third stage, potential associations obtained in the second stage were further assessed in 4694 independent individuals (2288 patients and 2406 controls).

2. Materials and methods

2.1. Subjects

The present study was approved by the Ethics Committee of each participating institute, and written informed consent was obtained from each participant. All participants were unrelated Japanese individuals.

The screening population in the first stage consisted of 340 patients with schizophrenia (180 men and 160 women; mean age, 41.8 [SD 14.9] years) and 426 control individuals (219 men and 207 women: mean age, 38.3 [SD 10.4] years). The expanded screening population in the second stage consisted of 595 patients with schizophrenia (313 men and 282 women; mean age, 40.2 [SD 14.1] years) and 598 control individuals (311 men and 287 women; mean age, 38.1 [SD 10.5] years). The expanded screening population included the screening population. The confirmatory population in the third stage consisted of 2288 patients with schizophrenia (1213 men and 1075 women; mean age, 46.5 [SD 14.4] years) and 2406 control individuals (1270 men and 1136 women; mean age, 45.9 [SD 13.9] years), and this population did not overlap with the expanded screening population.

We conducted a psychiatric assessment of every participant, as described previously (Watanabe et al., 2006). In brief, the patients were diagnosed according to the *Diagnostic and Statistical Manual of Mental Disorders Fourth Edition* (DSM-IV) criteria by at least two experienced psychiatrists, on the basis of all available sources of information, including unstructured interviews, clinical observations and medical records. The control individuals were mentally healthy subjects with no self-reported history of psychiatric disorders; they showed good social and occupational skills, but were not assessed using a structured psychiatric interview.

2.2. Genotyping

Initially, we screened 13 microsatellite markers on 22q with an average inter-marker interval of 2.63 Mb. All microsatellite markers were genotyped using an ABI 377 genetic analyzer (Applied Biosystems, Foster City, CA) with the GeneScan program v2.1 (Applied Biosystems), as described previously (Kaneko et al., 2007). The sequences of primers used for amplification are available upon request.

Next, we examined 25 tagging SNPs for *MYH9*, covering gene region and the 5′ and 3′ flanking regions (chr22:34996074... 35125125). These tagging SNPs were selected from the HapMap database (release #22, population: Japanese in Tokyo [JPT], minor allele frequency [MAF]: more than 0.05). We applied the criterion of an r^2 threshold greater than 0.8 in 'aggressive tagging: use 2- and 3-marker haplotype' mode using the 'Tagger' program (de Bakker et al., 2005), as implemented in Haploview v3.32 (Barrett et al., 2005). All SNPs were genotyped using the TaqMan 5′-exonuclease assay, as described previously (Watanabe et al., 2006). The sequences of probes used for the TaqMan assay are available upon request.

2.3. Statistical analysis

Deviation from the Hardy–Weinberg equilibrium (HWE) of microsatellite markers was tested using the GENEPOP v4.0.9 program (Rousset, 2008). The allele frequencies of microsatellite markers between patients and control individuals were compared using CLUMP v2.3 (Sham and Curtis, 1995). The number of simulations was 10,000 in each test, and the T1 statistic was adopted.

Deviations from the HWE for any of the SNPs were tested using the likelihood ratio test. Linkage disequilibrium (LD) blocks defined in accordance with Gabriel's criteria (Gabriel et al., 2002) and haplotype frequencies were determined using Haploview v4.01. The genotype, allele and haplotype frequencies of SNPs in patients and control subjects were compared using χ^2 test or Fisher's exact test. A probability level of $p<0.05$ was considered to indicate statistical significance.

A power calculation was performed using the Genetic Power Calculator (Purcell et al., 2003). Power was estimated with an α of 0.05, assuming a disease prevalence of 0.01 and the risk allele frequencies to be the values observed in control individuals.

3. Results

Initially, we examined 13 microsatellite markers on chromosome 22q in the screening population (Table 1). However, the alleles of AFM268YG1 (D22S1170) could not be precisely assigned. Mean heterozygosity for 12 markers was 0.747. The genotype distribution of no marker deviated significantly from the HWE in either group. We observed a potential association of

Please cite this article as: Amagane, H., et al., Failure to find an association between *myosin heavy chain 9, non-muscle* (*MYH9*) and schizophrenia: A three-stage case–control association study, Schizophr. Res. (2010), doi:10.1016/j.schres.2010.01.023

Table 1
Case–control association study of 13 microsatellite markers on 22q in the screening population.

Marker	Patients		Controls		Heterozygosity	Allelic p
	n	HWE	n	HWE		
AFM217XF4 (D22S420)	338	0.445	424	0.186	0.730	0.593
AFMA037ZD1 (D22S539)	337	0.503	424	0.107	0.529	0.144
AFM309WD5 (D22S1174)	325	0.585	398	0.638	0.822	0.675
AFM183XE9 (D22S315)	338	0.110	426	0.525	0.821	0.704
AFMA298YB5 (D22S1154)	338	0.157	417	0.305	0.520	0.907
AFMB294ZC1 (D22S1163)	335	0.651	423	0.533	0.718	0.192
AFM225XF6 (D22S280)	337	0.872	423	0.635	0.806	0.803
AFM168XA1 (D22S277)	339	0.253	426	0.697	0.866	0.608
AFM262VH5 (D22S283)	332	0.077	417	0.296	0.795	0.047
AFM261XD9 (D22S423)	339	0.722	425	0.888	0.787	0.318
AFM164TH8 (D22S274)	337	0.319	424	0.172	0.823	0.728
AFM268YG1 (D22S1170)		NA		NA	NA	NA
AFMB337ZH9 (D22S1169)	338	0.751	424	0.758	0.748	0.674

HWE, Hardy–Weinberg equilibrium; NA, not analyzed.

AFM262VH5 (D22S283) with schizophrenia (allelic $p = 0.047$), suggesting that there may be susceptibility loci for schizophrenia near this marker.

Because AFM262VH5 is located in intron 1 of *MYH9*, we investigated 25 tagging SNPs for *MYH9* in the expanded screening population (Table 2). The genotype distribution of no SNP deviated significantly from the HWE in either group. We found potential associations of rs1557538 (SNP#11) in intron 11, rs5756154 (SNP#15) in intron 5, and rs739096 (SNP#17) in intron 2 with schizophrenia (allelic $p = 0.021$, 0.023 and 0.020, respectively). In *MYH9*, five LD blocks were defined (Table 3). The haplotype 2–1–2 of block 4, which contained the minor allele of rs5756154, the major allele of rs11704382 and the minor allele of rs739096, was potentially associated with schizophrenia ($p = 0.024$).

To confirm the potential associations of rs1557538, rs5756154 and rs739096 with schizophrenia, we examined these SNPs in the confirmatory population (Table 4). However, we were unable to replicate these associations in the confirmatory population or a combined population comprising the expanded screening and confirmatory populations. Because rs5756154 (SNP#15) and rs739096 (SNP#17) were in LD, we

Table 2
Genotype and allele frequencies of 25 tagging SNPs in *MYH9* in the expanded screening population.

SNP #	db SNP ID	Allele[a]	Patients					Controls					p	
			n	1/1[b]	1/2[b]	2/2[b]	MAF	n	1/1[b]	1/2[b]	2/2[b]	MAF	Genotype	Allele
1	rs4821475	T/C	594	282	249	63	0.316	598	294	252	52	0.298	0.520	0.341
2	rs767855	C/T	593	498	92	3	0.083	598	500	94	4	0.085	0.983[c]	0.815
3	rs11703176	A/C	593	252	264	77	0.352	591	249	271	71	0.349	0.840	0.877
4	rs735854	C/T	595	354	214	27	0.225	596	348	218	30	0.233	0.885	0.642
5	rs5756129	C/T	592	311	226	55	0.284	595	309	239	47	0.280	0.610	0.831
6	rs5756130	C/T	595	470	119	6	0.110	597	474	118	5	0.107	0.961[c]	0.821
7	rs2239788	A/G	593	537	55	1	0.048	598	542	55	1	0.048	1.000[c]	0.963
8	rs5756133	T/A	595	443	139	13	0.139	594	465	120	9	0.116	0.265	0.100
9	rs2239781	T/C	593	233	270	90	0.379	597	239	270	88	0.373	0.958	0.767
10	rs3830104	T/C	593	430	149	14	0.149	597	425	154	18	0.159	0.741	0.504
11	rs1557538	A/G	594	349	217	28	0.230	596	391	182	23	0.191	0.051	0.021
12	rs9610489	C/T	595	280	261	54	0.310	598	286	256	56	0.308	0.932	0.899
13	rs2239784	C/T	594	428	152	14	0.152	598	429	159	10	0.150	0.666	0.900
14	rs1005570	G/A	595	482	109	4	0.098	598	482	110	6	0.102	0.889[c]	0.764
15	rs5756154	C/T	594	420	165	9	0.154	595	458	129	8	0.122	0.047	0.023
16	rs11704382	C/A	595	473	117	5	0.107	597	470	120	7	0.112	0.845[c]	0.667
17	rs739096	G/C	592	426	157	9	0.148	597	467	122	8	0.116	0.043	0.020
18	rs11089788	C/A	592	538	53	1	0.046	595	555	38	2	0.035	0.205[c]	0.170
19	rs9306310	G/A	595	518	76	1	0.066	598	533	63	2	0.056	0.431[c]	0.330
20	rs933224	T/C	595	406	170	19	0.175	598	412	163	23	0.175	0.754	0.998
21	rs6000262	A/G	595	396	181	18	0.182	597	407	165	25	0.180	0.363	0.885
22	rs2294356	C/A	595	458	125	12	0.125	598	454	130	14	0.132	0.877	0.615
23	rs5756168	T/C	595	499	91	5	0.085	597	516	77	4	0.071	0.431[c]	0.213
24	rs9610498	G/A	592	527	64	1	0.056	598	543	51	4	0.049	0.174[c]	0.483
25	rs11703137	G/A	595	303	247	45	0.283	598	330	223	45	0.262	0.306	0.238

SNP, single nucleotide polymorphism; *MYH9, myosin, heavy chain 9, non-muscle*; MAF, minor allele frequency.
[a] Major/minor alleles.
[b] Genotypes, major and minor alleles are denoted by 1 and 2, respectively.
[c] Calculated using Fisher's exact test.

Please cite this article as: Amagane, H., et al., Failure to find an association between *myosin heavy chain 9, non-muscle* (*MYH9*) and schizophrenia: A three-stage case-control association study, Schizophr. Res. (2010), doi:10.1016/j.schres.2010.01.023

Table 3
Haplotype analyses of five LD blocks in *MYH9* in the expanded screening population.

Haplotype	Patients	Controls	*p*
Block 1 (SNP #2–3–4)			0.863 [a]
1–1–1	0.648	0.650	0.908
1–2–2	0.142	0.148	0.683
1–2–1	0.128	0.118	0.430
2–2–2	0.082	0.085	0.828
Block 2 (SNP #5–6)			0.121 [a]
1–1	0.606	0.613	0.736
2–1	0.284	0.280	0.831
1–2	0.110	0.107	0.826
Block 3 (SNP #8–9)			0.252 [a]
1–1	0.619	0.625	0.740
1–2	0.243	0.258	0.381
2–2	0.137	0.115	0.117
Block 4 (SNP #15–16–17)			0.073 [a]
1–1–1	0.738	0.766	0.112
2–1–2	0.146	0.115	0.024
1–2–1	0.107	0.112	0.665
Block 5 (SNP #21–22–23–24–25)			0.376 [a]
1–1–1–1–1	0.718	0.732	0.443
2–2–1–1–2	0.122	0.128	0.653
1–1–2–1–2	0.084	0.068	0.153
2–1–1–2–2	0.055	0.046	0.335

LD, linkage disequilibrium; *MYH9, myosin, heavy chain 9, non-muscle*; SNP, single nucleotide polymorphism.
Major and minor alleles are denoted by 1 and 2, respectively.
[a] Global *p* values.

performed haplotype analyses of these SNPs (Table 5). In the expanded screening population, the haplotype 1–1, which was constructed from the major alleles of rs5756154 and rs739096, was significantly less frequent in patients than in control individuals ($p = 0.018$). By contrast, the haplotype 2–2, which was constructed from the minor alleles of these SNPs, was significantly more frequent in patients than in control individuals ($p = 0.024$). However, these associations could not be replicated in either the confirmatory or combined populations.

4. Discussion

Our three-stage case-control association study failed to find an association between *MYH9* within the 22q region and schizophrenia in the Japanese population. In the first stage, we examined 13 microsatellite markers on 22q to pinpoint genes for association analysis. There was a potential association of the marker AFM262VH5 in *MYH9* with schizophrenia. *MYH9* encodes the heavy chain of non-muscle myosin IIA (NMHC II-A), one of three NMHC II isoforms (A, B and C). The biological functions of NMHC II-A in the brain are poorly understood. Blebbistatin, which inhibits both NMHC II-A and -B, altered the structure of dendritic spines and decreased excitatory synaptic transmission (Ryu et al., 2006). Inhibition of NMHC II-B most likely underlay the morphological and functional abnormalities of spines caused by blebbistatin because *NMHC II-B* mRNA is predominantly expressed in the human brain among the three *NMHC* isoforms (Golomb et al., 2004), and because RNAi of *NMHC II-B* altered the structure of dendritic spines similarly to blebbistatin (Ryu et al., 2006). However, it could not be excluded that NMHC II-A may be implicated in regulation of the structure and function of spines. Interestingly, it has been reported that dendritic spine density is decreased in the brains of patients with schizophrenia (Glantz and Lewis, 2000; Rosoklija et al., 2000). Although further investigation will be needed, the role of NMHC II-A in the development of dendritic spines has possible relevance to schizophrenia.

Application of corrections for multiple testing decreases the probability of type I error (false positive), but increases that of type II error (false negative). Although the sample size of the expanded screening population was moderate, the power was only 0.12–0.49 when the genotypic relative risk was set at 1.4 for homozygous risk allele carriers under the multiplicative model of inheritance. To avoid inflation of the type II error probability, we did not apply corrections for multiple testing. Replication is essential for establishing the credibility of genetic associations (NCI-NHGRI Working Group on Replication in Association Studies, 2007). Therefore, possible associations observed in the moderate-scale population were further assessed in the large-scale independent population. However, we were unable to replicate these associations. The nominally significant associations in the first and second stages were most likely the results of type I error. It is unlikely that the negative results in the third stage were caused by type II errors because the power was more than 0.8 in the confirmatory population. There is another possible explanation for the discrepancy between the results in the

Table 4
Genotype and allele frequencies of three SNPs in *MYH9* in the confirmatory and combined populations.

db SNP ID	Patients					Controls					*p*	
	n	1/1 [a]	1/2 [a]	2/2 [a]	MAF	*n*	1/1 [a]	1/2 [a]	2/2 [a]	MAF	Genotype	Allele
rs1557538												
Confirmatory	2233	1370	762	101	0.216	2375	1471	790	114	0.214	0.776	0.858
Combined	2827	1719	979	129	0.219	2971	1862	972	137	0.210	0.301	0.233
rs5756154												
Confirmatory	2257	1658	555	44	0.142	2359	1728	585	46	0.144	0.987	0.886
Combined	2851	2078	720	53	0.145	2954	2186	714	54	0.139	0.624	0.377
rs739096												
Confirmatory	2268	1706	521	41	0.133	2380	1783	555	42	0.134	0.957	0.853
Combined	2860	2132	678	50	0.136	2977	2250	677	50	0.131	0.659	0.381

SNP, single nucleotide polymorphism; *MYH9, myosin, heavy chain 9, non-muscle*; MAF, minor allele frequency.
[a] Genotypes, major and minor alleles are denoted by 1 and 2, respectively.

Please cite this article as: Amagane, H., et al., Failure to find an association between *myosin heavy chain 9, non-muscle* (*MYH9*) and schizophrenia: A three-stage case-control association study, Schizophr. Res. (2010), doi:10.1016/j.schres.2010.01.023